2018

The Characterization of RNA Content and Biogenesis Pathways of Extracellular Vesicles That Have Been Implicated in the Pathogenesis of HIV-1 Associated Neurocognitive Disorders

Virginia Elizabeth Zwikelmaier
Loyola University Chicago

LOYOLA UNIVERSITY CHICAGO

THE CHARACTERIZATION OF RNA CONTENT AND BIOGENESIS PATHWAYS OF EXTRACELLULAR VESICLES THAT HAVE BEEN IMPLICATED IN THE PATHOGENESIS OF HIV-1 ASSOCIATED NEUROCOGNITIVE DISORDERS

A THESIS SUBMITTED TO

THE FACULTY OF THE GRADUATE SCHOOL

IN CANDIDACY FOR THE DEGREE OF

MASTER OF SCIENCE

PROGRAM IN INFECTIOUS DISESASE AND IMMUNOLOGY

BY

VIRGINIA ZWIKELMAIER

CHICAGO, ILLINOIS

AUGUST 2018

TABLE OF CONTENTS

LIST OF FIGURES

CHAPTER ONE

OVERVIEW AND HYPOTHESIS

Although modern-day combined anti-retroviral therapy (cART) potently suppresses the replication of human immunodeficiency virus type 1 (HIV-1), patients still suffer from a variety of neurological, behavioral, and motor dysfunctions collectively referred to as HIV-1 Associated Neurocognitive Disorders (HAND).[1–3] While not as severe as the HIV-1 Associated Dementia (HAD) that inflicted those in the pre-cART era—whose uncontrolled infection had progressed to Acquired Immune Deficiency Syndrome (AIDS)—the milder HANDs still impact these patients' quality of life.[3,4] Current research suggests the manifestations of HAND are not due to local replication of the virus in the brain, but the chronic activation of infected microglial cells and astrocytes, and the dissemination of toxic HIV-1 components throughout the brain by way of extracellular vesicles (EVs).[5–9] The combination of this chronic pro-inflammatory environment and the transfer of these pathogenic components to neurons, leading to neuronal dysfunction and death, are proposed to be the cause of the neuropathology observed in HAND.[5–9] In this thesis, I aimed to gain a better understanding of the specific populations of EVs that potentially contribute to HAND.

The first goal of this thesis was to develop a method to assess the microRNA (miRNA) content of EVs at an individual level. Both viral miRNAs and virally-dysregulated host miRNAs have been detected in EVs released from HIV-1 infected cells.[10–12] Furthermore, these miRNA-

containing EVs have negative effects on neurons and other cells of the brain, implicating them as potential sources of neuropathogenesis in HAND.[11,13,14] A variety of techniques are used in the field to look at the miRNA content of EVs including RT-PCR, RNA-seq, other next-generation sequencing methods, and mass spectrometry. While these methods are invaluable in assessing the larger trends in whole EV populations, they cannot distinguish specifics between the many subpopulations that exist in these highly heterogenous EV mixtures. Development of a way to look at the RNA content of a single EV would allow the characterization of distinct populations and potentially aid in the understanding of the targeted incorporation of specific RNA species into such populations. Could a molecular probe be used to assess the miRNA content of an individual EV? I hypothesized that if a molecular probe could indeed detect a specific miRNA within an individual EV, then I would expect to see co-localization of the probe signal with EV markers. To test this, I combined the use of a molecular beacon with our wide-field deconvolution fluorescence microscopy imaging technique, which facilitates the individual analysis of thousands of EVs simultaneously.

The second goal of this thesis was to investigate the potential differences in the biogenesis of EVs that contain the HIV-1 viral proteins Tat, Nef, and Vpr. These proteins have been found to be secreted and often associated with EVs.[12,15–17] Moreover, each of these proteins has a multitude of adverse effects when expressed in or taken up by neurons and other cells of the brain.[17–20] Characterization of these HIV-1 protein-containing EV populations would provide a foundation in understanding the EV-mediated mechanisms that contribute to the pathology of HAND. Previous work in our laboratory began to evaluate these populations through a marker-based strategy and observations from this study of the differences in the

markers between these three proteins prompted a deeper look into how these different EV populations were formed. Could these EVs have different biogenesis mechanisms? I hypothesized that if EVs containing different HIV-1 proteins arise from different biogenesis pathways, then manipulation of components of one pathway would alter the EV flux for one of the three proteins, but not the others. While analysis of EVs released from cells infected with HIV-1 would be the most physiologically relevant and most applicable in a disease-state model, this would require the separation of the newly produced viruses from the EVs. Unfortunately, virions and EVs are nearly identical in their physical and chemical characteristics and share many of the same biogenesis mechanisms. With current isolation techniques, there is no reliable method to completely and consistently separate the two. As such, these studies have been carried out by stably expressing Tat, Nef, and Vpr (either individually or in combination) in cells, altering the unconventional autophagic EV secretion pathway through drug manipulation, and analyzing the EVs that are released. In an effort maintain some form of physiological relevance, these studies use a human microglial cell line (C20), an improvement over our previous studies that primarily used human embryonic kidney cells (HEK293T).

The next chapter will acquaint the reader with the pertinent literature. It begins with a general review of HIV-1 and its Central Nervous System (CNS) involvement, followed by a brief history of anti-retroviral therapies and a more detailed look at HAND. The focus then shifts to EVs, with an explanation of what they are and their roles in normal physiological function before concentrating on their pathogenic potential in various diseases and emphasizing their functions in HAND pathogenesis. The chapter ends with a discussion on EV nomenclature and

the ties of the nomenclature to EV biogenesis, before closing with descriptions of three different EV biogenesis pathways.

CHAPTER TWO

REVIEW OF THE LITERATURE

Human Immunodeficiency Virus I

Human immunodeficiency virus type 1 (HIV-1) was first discovered in 1983 as the etiologic agent of Acquired Immune Deficiency Syndrome (AIDS).[21] Responsible not only for the United States AIDS epidemic of the 1980s, but also the ongoing global AIDS pandemic, HIV remains a pervasive threat to health worldwide. Since its discovery, over 76 million people have become infected with HIV and it is estimated there are 36.7 million people currently living with HIV, with approximately 1.8 million new cases occurring annually.[22]

Transmitted primarily through sexual contact, HIV-1 first invades mucosal surfaces, spreading to regional lymph nodes and replicating in the gut-associated lymphoid tissues (GALT), before entering the bloodstream and becoming a systemic infection.[23] While Langerhans and other dendritic cells (DCs) play important roles in initial HIV-1 invasion and dissemination, HIV-1 primarily infects three types of immune cells: macrophages, microglia, and CD4+ T cells. Infection of these cell types is dependent on their expression of the cell surface glycoprotein CD4, and chemokine receptors such as CCR5 or CXCR4, which serve as the receptor and co-receptors, respectively, for HIV-1.[1] Sequential binding of the gp120 portion of HIV-1's trimeric envelope spike protein to both CD4 and either co-receptor leads to fusion of the viral envelope with the plasma membrane, mediated by the gp41 portion of the spike

protein. Fusion of these membranes results in the release of the conical viral core into the cytoplasm.[1] As the viral core is trafficked to the nucleus, HIV-1 reverse transcribes its RNA genome into double-stranded DNA. After import into the nucleus, this DNA is integrated into the host genome by a virally encoded integrase. When this integration site is transcriptionally active, short transcripts encoding regulatory proteins are initially produced to aid in the production of longer RNA transcripts, which ultimately leads to the translation of viral components, replication of the viral genome, and assembly of new virions at the cytoplasmic side of the plasma membrane.[1] These new virions bud off from the plasma membrane and become mature, infectious HIV-1 particles upon cleavage of gag polyproteins by a viral protease to form the structured, conical capsid.

AIDS, the late stage of HIV infection, prompts the appearance of opportunistic infections and reactivation of latent infections, key indicators of immunosuppression. Roughly 35 million people have died from AIDS-related illnesses since the worldwide spread of HIV began.[22] The cause of this severe immunosuppression during the later stages of HIV infection is intimately linked to the viral lifecycle of HIV, and the consequences of the host's immune response to the virus. Initial invasion of the mucosa and spread to the local lymphatics is referred to the eclipse phase of HIV infection. During this phase, there is no viral RNA detectable in the blood, and thus a blood test would read as negative. HIV is far from idle, however, as it during this phase a large decline in CD4+ T cells occurs as the high concentration of resident CD4+ T cells in the GALT succumb to infection, facilitating massive HIV replication.[24] Systemic spread of HIV in the acute phase of infection presents nonspecifically as a flu-like syndrome and is characterized by high viral loads in the blood. Despite the cytokine storm brought on by the general anti-viral

response, both innate and adaptive effectors are unable to fully control infection. Natural Killer (NK) cells and CD8+ cytotoxic T cells are able reduce the viral load by killing infected cells, but initial antibody responses are non-neutralizing.[23,24] The high mutation rates of HIV, a result of the lack of proofreading machinery involved in reverse transcription of HIV's genome, makes the neutralizing antibodies that do arise four months post-infection, largely ineffective.[23,24] With the inability to completely clear the virus, HIV becomes an asymptomatic, chronic infection, maintaining high levels of replication and slowly depleting the host's CD4+ T cells over the course of years. When the patient's CD4+ T cell count drops below 200 cells/mm^3, the clinical presentations of AIDS begin to manifest. The majority of those infected with HIV-1 die not from primary HIV infection, but from the secondary infections and complications that result from the many years of chronic inflammation and a severely weakened immune system.

HIV-1 and the Central Nervous System.

Early in primary HIV-1 infection, when the virus has spread systemically, HIV-1 RNA can be detected in the Cerebral Spinal Fluid (CSF), indicating the virus has invaded the Central Nervous System (CNS).[25] How HIV-1 is initially crossing the Blood-Brain Barrier (BBB), a semi-permeable membrane that highly selectively restricts access of circulating substances to the brain, is not fully understood. A well-accepted "Trojan horse" hypothesis suggests HIV-1 crosses the BBB by hiding within circulating CD4+ T lymphocytes and monocytes that enter the CNS during routine surveillance.[25,26] This is supported in part by recent evidence that HIV-1 infection can alter monocyte cell surface protein expression to increase their transmigration across the BBB.[27] Another theory involves "cell-free" crossing of HIV-1 due to decreased BBB integrity. Inflammatory cytokines such as tumor necrosis factor α (TNF-α), interleukin-1β (IL-1β), and

interleukin-16 (IL-16), are known to increase permeability of the cerebral endothelial cells that form the BBB, disrupting of the tight junctions that keep this restrictive barrier together.[28,29] With the chronic and systemic immune activation and pro-inflammatory environment HIV-1 infection creates, the lessened stability of the BBB enhances the entry of free virus into the brain.[30] Additionally, HIV-1 has been shown to be use vesicular transport to enter the brain, being transcytosed by the endothelial cells of the BBB.[31]

As a more "immunologically unique" environment, invasion of the CNS offers HIV-1 more protection and evasion from the host's conventional immune system, with access of most innate and adaptive immune effectors to the CNS being greatly restricted. However, this means that HIV-1 has less access in this area to its primary target cell, the CD4+ T lymphocyte, to support replication. Most cells of the brain, including neurons and oligodendrocytes, cannot be infected by HIV-1.[25,32] Astrocytes, it appears, can become infected with HIV-1, but cannot support a productive infection.[28,32] Perivascular macrophages, other non-parenchymal brain macrophages, and microglial cells, which all express low levels of CD4 but high levels of the chemokine co-receptors, become HIV-1's main targets in the CNS.[5,28] Unlike HIV-1 infection of CD4+ T cells which, if not latent, quickly leads to apoptotic or pyroptotic death of the host cell, productive infection of these cells can be sustained for longer periods of time.[23,28,33]

Despite HIV-1's early entry into the CNS and the elevated levels of inflammatory cytokines and markers detected in the CSF, most patients remain neurocognitively asymptomatic or subclinical for many years, with severe HIV-1 Associated Dementia (HAD) only presenting late in HIV-1 infection.[2,25] Characterized by severe memory loss, delirium, confusion, speech impairment, apathy, and debilitating motor dysfunctions, HAD was reported in 30 to 60

percent of AIDS patients prior to modern therapies.[2,25,32] These late-stage symptoms are attributed to the neuropathology of underlying HIV-1 associated encephalitis (HIVE) which includes virally-induced fusion of microglia and/or macrophages into multinucleated giant cells, formation of inflammatory nodules of activated microglia around necrotic brain tissue, damage to astrocytes and myelin sheaths, and ultimately neuronal cell death.[5,30,32]

Combating HIV-1: Anti-Retroviral Therapy

Since its discovery, countless researchers have put forth massive efforts to understand HIV-1 in order to control and combat it. The first drug therapies targeted one of the key features of the retrovirus: the reverse transcriptase. Drugs that acted as nucleoside reverse transcriptase inhibitors (NRTIs) were the first to hit the market, although they had varying degrees of success and each had their own associated toxicities and side effects.[34,35] Another issue was HIV's rapidly mutating genome would quickly evolve resistance to a certain NRTI, which lead to therapy regimens that alternated use of each NRTI, and later regimens that combined them.[34] Effective control of HIV-1 was not seen until the development of non-nucleoside reverse transcriptase inhibitors (NNRTIs) and protease inhibitors in the mid-1990s. By targeting not only the reverse transcription step in HIV-1's life cycle through combinations of NRTIs and NNRTIs, but also the final maturation step through protease inhibitors, this highly active anti-retroviral therapy (HAART) was able to potently suppress HIV-1 replication and turn HIV-1 infection from a death sentence into a chronic, but manageable, condition.[1,34,36] Since then more drugs for modern combination anti-retroviral therapy (cART) have become available, targeting other steps in the HIV-1 life cycle such as viral entry/attachment and proviral integration.[34,37] Improvements in assays to more accurately measure plasma HIV-1 RNA and

CD4+ T cell levels have allowed better assessment of disease stage and progression, and the ability to genetically profile for HIV-1 drug resistances has allowed for more personally optimized treatment options.[1] A recent shift in cART initiation protocol, from starting treatment when nearing AIDS status to starting as soon as a patient tests HIV positive regardless of CD4+ T cell count, along with prophylactic treatments for partners of infected individuals to reduce the risk of contracting the virus, has greatly improved the outlook for those infected with HIV-1.[38,39]

Despite these successes, long-term use of these drugs has been associated with the development of multiple comorbidities including heart disease, liver disease, diabetes, and various cancers.[35,40,41] Additionally, current cART effectively controls infection, but cannot cure it. Consequently, strict adherence to cART is absolutely required as it suppresses viral replication and production of new virus but does not eliminate integrated and latent proviruses, so cessation of therapy can lead to rapid viral rebound from latently infected cell reservoirs. Unfortunately, cART is incredibly expensive and not widely accessible in less-industrialized parts of the world.[1,34] Of the 36.7 million people infected with HIV, only about 50 percent have access to cART, and only a fraction of those are able to consistently adhere to the regimens for longer term.[22]

HIV-1 Associated Neurocognitive Disorders.

With the advent of these potent therapies, AIDS-related fatalities and incidence of the severe neurological and motor deficits of HAD drastically declined.[3] However, HIV-1 patients exhibit an array of neurocognitive, behavioral, and motor dysfunctions, even when adhering to cART.[4] Collectively referred to as HIV-1 Associated Neurocognitive Disorders (HAND), this group of complications includes a wide spectrum of manifestations that is subdivided into three main

classifications: asymptomatic neurocognitive impairment (ANI), mild neurocognitive disorder (MND) or mild-motor neurocognitive disorder (MMND), and lastly the most severe global impairments remain classified as HAD.[3,42] While cART reduced the incidence of HAD in HIV-1 patients, these less severe but still life-impacting manifestations have become more prevalent and are in seen in up to 50 percent of those compliant to cART.[3,4]

The cause for this apparent uptick in milder HAND presentations was perplexing and still has not been completely resolved. With evidence that cART achieved systemic viral suppression, initial thoughts went to poor drug penetrance into the more inaccessible regions of the CNS. With conflicting evidence of continued viral evolution in the CNS and data indicating cART greatly decreases HIV-1 RNA levels in the CSF, whether poor drug penetrance contributes to HAND remains up for debate.[26,28,43–46] Also controversial is the correlation of viral RNA level in the CSF with manifestations of neurocognitive impairment (NCI), particularly since higher viral loads have been observed in post-mortem brains than in the CSF of patients who have varying degrees of NCI.[30,44,46,47] Additionally, post-mortem assessments of brain tissue found HIV-1 replication to be highly localized, with only a small fraction of resident microglial cells infected with HIV-1, suggesting local viral replication is not the main cause of the widespread neuropathology observed in HAD or milder HANDs.[5,48,49] More recent studies point to chronic inflammation in the brain as the culprit of HAND, through not only the production and release of soluble pro-inflammatory cytokines and reactive oxygen species (ROS) by activated macrophages, microglia, and astrocytes, but also the trafficking and delivery of HIV-1 components harbored in extracellular vesicles.[5–9] These components have negative effects on

neurons by altering neuronal metabolic function, signaling, electrochemistry, and lead to neuronal death.[14,50,51]

Extracellular Vesicles and Their Cargo

Extracellular vesicles (EVs) were originally thought to merely contain jettisoned cellular waste or to simply be a byproduct of apoptotic blebbing, but have since been found to be crucial to normal physiological intercellular communication.[52,53] Involved in routine cell-cell signaling events, including tissue development and immune responses, and shown to be protective against tissue injury and microbial infection, these small vesicles play an important role in the overall health of an organism.[54–59] However, like all cellular processes, this system of intercellular communication can be altered and negatively impact the organism. EV formation and cargo-loading can become dysregulated, contributing to disease pathogenesis, tumor maintenance and metastasis, and facilitating microbial infection.[7,10,60–63]

Of great interest is the cargo EVs carry, both in their lumen and on their surface. EVs can contain a variety of physiologically relevant proteins, carbohydrates, nucleic acids, and specialized lipids, and are specifically enriched in a subfamily of proteins involved in the organization of membrane microdomains, called tetraspanins.[52,53,64,65] Tetraspanins such as CD9, CD63, and CD81 are among the most commonly found tetraspanins in EVs released from a variety of tissues and thus are the most widely recognized “canonical” EV markers.[53,66,67] The other cargoes EVs carry, particularly microRNAs and tissue- or pathogen-specific proteins, have become the focus in many fields in the use as “biomarkers” in the assessment of disease progression.[68,69]

MicroRNAs.

MicroRNAs (miRNAs or miRs) are small, roughly 22-nucleotide long sequences of non-coding RNA that participate in post-transcriptional regulation of gene expression by targeting specific messenger RNAs (mRNAs) for degradation or repression.[70] Many different miRNAs have been found to be involved in cell differentiation, proliferation and death, tissue development and homeostasis, and metabolism, and are differentially expressed both spatially and temporally.[70,71] Dysregulation of miRNAs has been linked to various diseases including many types of cancers, microbial infections, as well as metabolic and neurological disorders.[71–73] The pathological consequences of these dysregulations have been particularly observed in association with EVs, both in the targeted depletion of certain miRNAs from cells via packaging into and subsequent ejection of EVs, and the transfer of certain miRNAs to other cells through fusion of EVs with cellular membranes.[7,14,74–76]

Pathogenic Proteins.

The trafficking of proteins with pathogenic effects from cell to cell through EVs has been observed most notably in the proteopathies of the brain. The spread and transfer among neurons of misfolded protein aggregates, such as amyloid-β (Aβ) and α-synuclein (α-syn), are responsible for the neuropathogenesis observed in Alzheimer's Disease (AD) and Parkinson's Disease (PD), respectively.[77] Higher-order oligomerization of proteins has been observed to be an indicator of targeted EV cargo-loading, so it comes as no surprise that both Aβ and α-syn have been found associated with EVs, and these EVs have been shown to transfer these aggregated proteins to new cells, leading to neuronal dysfunction.[60,61,78,79] Additionally, tau,

another aggregating protein important in the neuropathology of both AD and PD, has been found in and to be transferred by EVs.[80,81]

Cargo Implicated in HIV-1 Associated Neurocognitive Disorders.

As indicated earlier, EVs are speculated to be major players in the widespread neuropathology of HAND. HIV-1 components, including viral proteins and RNAs, as well as dysregulated host RNAs have all been observed to have cytopathic effects on neurons and other cells of the brain. These pathogenic factors have increasingly been found to be incorporated into the EVs released from virally infected cells.

Viral and Host miRNAs. The virally encoded *trans*-activation response element (TAR) RNA, a crucial component involved in HIV-1 genome amplification, has also been discovered to be processed into miRNAs (miR-TARs).[10,12] These miR-TARs promote an anti-apoptotic state in the infected cell by downregulating the expression of pro-apoptotic factors.[10] Additionally, TAR RNA and these miR-TARs have been detected in EVs, along with host miRNA processing machinery, and have been reported to induced both an anti-apoptotic and a pro-inflammatory state on target cells.[10,12] Other virally-derived miRNAs (vmiRs), vmiR-88 and vmiR-99, were found to enhance expression of the pro-inflammatory cytokine TNF-α in macrophages and could be detected in EVs isolated from the sera of HIV-1 positive patients.[11]

Host cell miRNAs have been shown to play important roles in the anti-viral response against HIV-1 by targeting viral RNAs for cleavage and degradation.[76] To combat this, HIV-1 has developed ways to alter host miRNA expression profiles, either through up- or downregulation at the transcriptional level, or through deregulation of miRNA incorporation into EVs.[13,14,72,76,82,83] While preventing suppression of the virus in the infected cell, these EVs

containing re-directed miRNAs can have negative effects on surrounding cells. Expression of HIV-1 proteins in astrocytes has shown increased secretion of miR-29 and miR-132 in EVs and delivery of these miRNAs to neurons has been linked to neurite shortening and neuronal death.[13,14]

Tat. The *trans*-Activator of Transcription (Tat) protein, is a small 86-102 amino acid protein that is essential for successful HIV-1 viral replication. Among the early genes encoded by the HIV-1 genome, Tat interacts with HIV-1 TAR RNA and recruits host cell factors to drive the phosphorylation of RNA polymerase II in a positive feedback loop to greatly increase the production of longer HIV-1 RNA transcripts.[18] Tat has also been shown to be able to translocate across cellular membranes and is unconventionally secreted from infected cells, potentially via pore formation.[15,84] When taken up by nearby cells, Tat has been reported to have a variety of effects on these "bystander" cells, including upregulating co-stimulatory molecules on DCs and monocytes, upregulating the HIV-1 coreceptors CXCR4 and CCR5 on CD4+ T cells, and also directly causing CD4+ T cell apoptosis.[15,85]

In the CNS, Tat causes pro-inflammatory activation and dysfunction of microglial cells and astrocytes, as well as altering cell cycle and triggering cell death in astrocytes.[18,86] Tat is particularly toxic to neurons, shown to dysregulate synaptic activity, decrease neurite length, and ultimately lead to neuronal death.[13,18,87] Additionally, Tat alters the process of autophagy in neurons, which as terminally-differentiated cells, has severely detrimental consequences.[18,50] Recently, Tat has been detected in EVs, and neurons treated with these Tat-containing EVs collected from CD4+ T cells and astrocytes showed similar phenotypes to those as previously reported with recombinant Tat studies, with increased neurite shortening and decreased

neuronal cell survival.[16] This suggests these Tat-containing EVs are biologically active and have the potential to be among the factors contributing to HAND.

Nef. Negative Regulatory Factor (Nef) is another protein expressed early on during HIV-1 infection. Despite possessing no enzymatic activity, this 27-35 kDa protein is highly active and multifunctional.[88] Nef has been found to downregulate critical T cell signaling surface proteins, including CD4, CD28, MHC class I, and the TCR/CD3 complex, while simultaneously triggering signaling cascades that mimic TCR-stimulation leading to dysregulated T cell activation.[88] With a domain on its N-terminus that is myristoylated, a post-translational lipid modification, Nef is able to associate with cellular membranes. This membrane anchor has been noted to enhance the targeted loading of proteins into EVs and thus myristoylated Nef was found in EVs early on and has been observed to greatly enhance both viral and EV particle release.[12,89] Nef also appears to have some function in viral infectivity, as Nef-deficient virions are less infectious.[88] Lastly, Nef appears to be involved in suppression of host RNA silencing factors that target HIV-1.[76,90]

Nef-containing EVs have been noted to induced apoptosis in CD4+ T cells and recombinant Nef was shown to activate microglial cells into a pro-inflammatory state.[19,91] Nef also alters the function of autophagy in both macrophages and astrocytes.[20,92] And finally Nef-containing EVs have been reported to cause the secretion of Aβ fibrils from neurons and can lead to neuronal death.[20,93] All of these neurotoxic functions are possible indications that Nef-associated EVs may be contributing to HAND pathology.

Vpr. The Viral Protein R (Vpr) is a 14 kDa accessory protein that is part of the HIV-1 pre-integration complex (PIC) and is essential for infection of non-dividing cells.[94] Vpr is a

multifunctional protein and aside from nuclear import of the viral genome, has roles in mediating cell cycle progression and can influence the accuracy of the reverse transcription step of HIV-1 replication, altering the viral mutation rate.[17,94] In proliferating cells, Vpr induces cell cycle arrest in G2 phase.[94] Interestingly, Vpr can act in a pro-apoptotic or an anti-apoptotic manner depending on the cell type. Vpr induces apoptosis in DCs, monocytes, and neurons, while it prohibits apoptosis in macrophages and microglial cells.[17,92] In T lymphocytes, Vpr's function has been controversial as both the pro-apoptotic and anti-apoptotic behaviors have been observed.[92,94]

Beyond its apoptotic effects, Vpr has been shown to activate pro-inflammatory states in macrophages, microglia, and astrocytes, and alter the electrochemistry of neurons.[17] Due to Vpr's penchant for causing cell cycle arrest and apoptosis, *in vitro* studies with Vpr-expressing cell lines are difficult. Vpr has been detected in supernatants collected from virally infected cells but while Vpr is speculated to be an EV-associated player in HAND, no published studies have shown the presence of Vpr in EVs thus far.[10,17]

Extracellular Vesicle Biogenesis

Nomenclature is a much-debated topic in the world of EVs, with disagreements on what specifically qualifies as an "exosome" versus a "microvesicle" or "ectosome" or "ejectosome" or "microparticle", and so on.[52,95] Much of the problem stems from the plethora of terms used to describe the same type of vesicle when isolated from different cell types, tissues, or bodily fluids.[52,95] Limitations in differentiating EV types combined with the fact that in many studies stringent assessment of the type of EVs collected is not preformed, lead to lenient misuse of many of the classifications.[52] While these distinctions may be ambiguous and perhaps arbitrary,

these attempts to categorize the different types of EVs may offer some insight on differences in their biogenesis pathways.[66] These differences can in turn provide a greater understanding of heterogeneous EV populations, as well as how certain subsets of EVs can become potential vehicles for pathogenesis. Focused on here are three main pathways: budding from the plasma membrane, release from multivesicular bodies, and unconventional autophagic secretion.

Plasma Membrane Budding: Microvesicles and Ectosomes.

EVs that bud directly from the plasma membrane have been referred to by a great number of names, but are primarily called microvesicles or ectosomes (Figure 1A).[52] While the exact size range for these vesicles is not fully agreed upon, the general consensus is that these EVs can range from a diameter of 50 nanometers to a few microns.[52,64,65] The biogenesis mechanisms of these EVs are not well characterized but appear to involve the clustering of specialized phospholipids in a microdomain as well as the repositioning of phosphatidylserine to the outer leaflet of the plasma membrane by lipid translocases, although this is also a characteristic of another type of EV, apoptotic bodies, which are typically larger and only produced during apoptosis.[64,65] The actin-myosin cytoskeleton is also involved in this process, with activated ADP-ribosylation factor 6 (ARF6) causing a signaling cascade that results in cytoskeletal contraction.[64] Influx of calcium and hypoxia have also been observed to trigger EV release from the plasma membrane, although the underlying mechanisms are not understood.[65] Curiously, TSG101—a protein that is part of the machinery for endosomal vesicle formation—was reported to be recruited to the plasma membrane and be detected within these EVs.[52] Additionally, the tetraspanins CD9, CD63, and CD81 were initially thought be specific markers of endosomally-derived EVs and play a role in their endosomal biogenesis, but

recent studies have shown these proteins are also found in EVs derived from the plasma membrane.[67]

Exosomes and Multivesicular Bodies.

Exosomes are small EVs that range in diameter from 30-150 nanometers, with an endosomal origin that is characterized by the formation of multivesicular bodies (Figure 1B).[52,64,65] Being vesicles themselves, endosomes are formed by invagination of the plasma membrane during endocytosis.[65] These early endosomes become either recycling endosomes, to which cellular components to be recycled are targeted, or late endosomes, to which cellular components to be degraded or exocytosed are targeted.[65] It is these late endosomes that serve as the sites for exosome biogenesis, which first requires enrichment of the endosomal membrane with tetraspanins and the recruitment of four protein complexes, the endosomal sorting complexes required for transport (ESCRT).[65] The first ESCRT complex, ESCRT-0, is responsible for recognizing and sequestering ubiquitinated cargo.[65,67] The next two complexes, ESCRT-I and -II, are involved in the inward budding of the endosomal membrane with the sequestered cargo.[67] The last complex, ECSRT-III, causes the final scission of the budding exosomes-to-be, forming intralumenal vesicles (ILVs).[65,67] Endosomes containing ILVs are referred to as multivesicular bodies (MVBs) or multivesicular endosomes (MVEs). These MVBs are then targeted to the lysosome for degradation or are sent to the plasma membrane (Figure 1C -D).[52] Upon fusion with the plasma membrane, the ILVs are released into the extracellular space and are now referred to as exosomes (Figure 1E).

While this ESCRT-dependent pathway is accepted as the canonical exosome biogenesis pathway, ESCRT-independent pathways have also been observed. In ESCRT-depleted systems,

CD63 positive exosomes are still produced, suggesting the tetraspanins themselves play a role.[52] Proteoglycans and adaptor proteins, such as syndecan and syntenin, along with sphingomyelinase also appear to have roles in the ESCRT-independent generation of exosomes.[52,65]

Unconventional Autophagic Secretion.

EV release through unconventional autophagic secretion is a newer concept, the mechanisms of which are poorly understood. Discovered as a way cytosolic proteins like IL-1β, IL-18, and HMGB1 (which all lack secretion peptide signals) are secreted, unconventional secretion involves a specialized form of macroautophagy, called secretory autophagy.[96,97] It is currently unclear if secretory autophagosomes arise from a completely separate mechanism than classical degradative autophagosomes, or if the two share a common precursor.[96] Recent studies potentially indicate the latter, as factors involved in degradative autophagy, Atg5 and Rab8a, have been found to be involved in the secretion of IL-1β in this unconventional autophagic manner.[96,98] Additionally, elongation and closure of the double membranes appears to require lipidation of LC3 for both degradative and secretory autophagosomes.[96,98] However, initial secretory autophagosome formation requires GRASP55 and GRASP65, instead of the enrichment of Atg14 and phosphatidylinositol 3-phosphate (PI3P) that are required for initial degradative autophagosome formation.[96]

Regardless of how these autophagosomes are formed, both have the capacity to fuse with MVBs, forming amphisomes (Figure 1F).[96] These amphisomes then fuse with their parent autophagosome's intended target, the lysosome or the plasma membrane (Figure 1G-H). Fusion of an amphisome with the plasma membrane results in the release of ILVs as EVs (Figure

1I).[96] While EV release in this way has been observed, how it is happening is still controversial. The logistics of the fusion of these double-membraned amphisomes with the plasma membrane in regards to the location of the ILVs has yet to be established.[96] While likely sharing a similar biogenesis mechanism to exosomes due to the shared generation of MVBs, the autophagic component of this pathway potentially means these EVs carry distinct markers and cargo not observed in classical exosomes.[99,100]

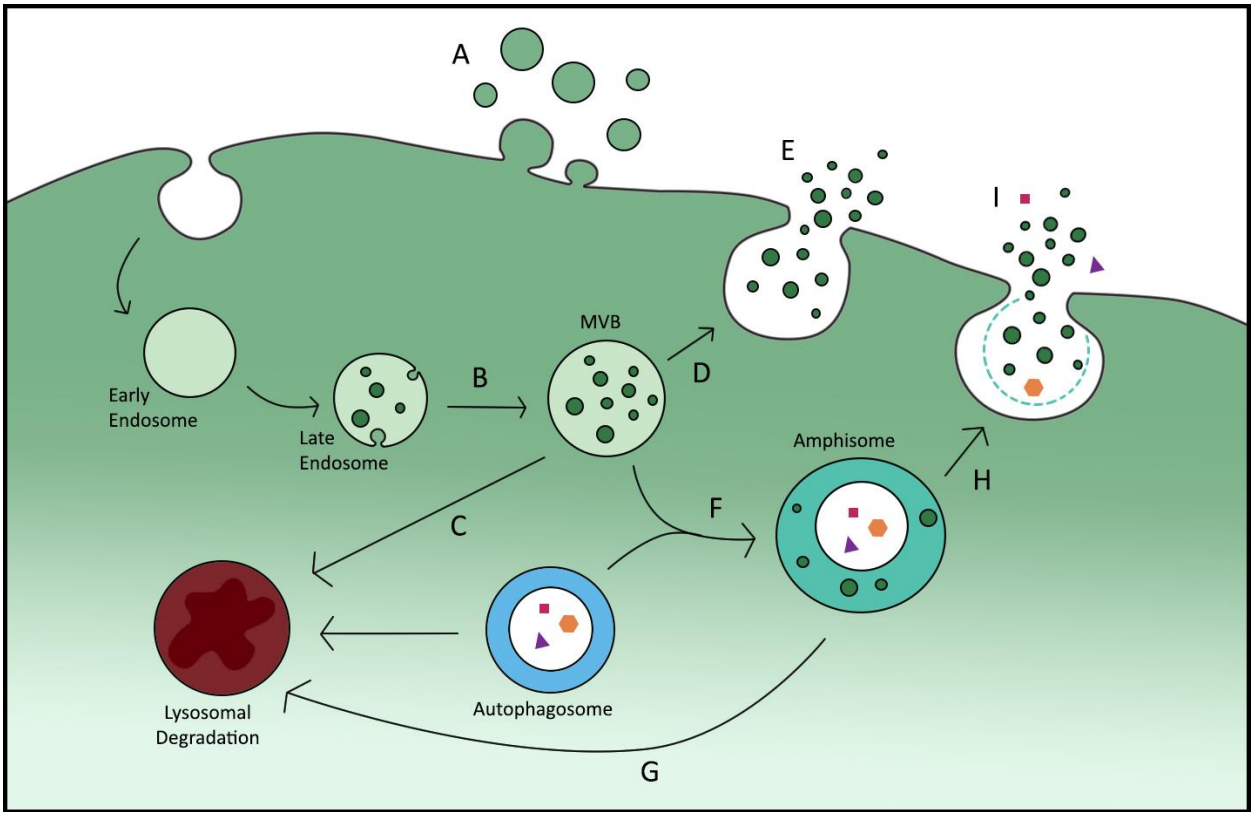

Figure 1. **Extracellular Vesicle Biogenesis and Release Pathways.** An illustration of the pathways of extracellular vesicle formation and release. **(A)** The budding from the plasma membrane of microvesicles and ectosomes. **(B)** The inward budding of intraluminal vesicles (ILVs) into late endosomes to form multivesicular bodies (MVBs). **(C)** The targeting of MVBs for degradation to lysosomes. **(D and E)** The targeting of MVBs to and fusion with the plasma membrane, releasing the ILVs as exosomes. **(F)** The fusion of an MVB with an autophagosome to form an amphisome. **(G)** The targeting of amphisomes to lysosomes for degradation. **(H and I)** The targeting of amphisomes to and fusion with the plasma membrane, releasing the ILVs and autophagic contents into the extracellular space, termed unconventional autophagic secretion.

CHAPTER THREE

MATERIALS AND METHODS

Detection of MicroRNAs in Individual Extracellular Vesicles with a Molecular Beacon

Cell Culture.

HEK293T (293T) cells were cultured at 37 degrees Celsius and 5 percent Carbon Dioxide in Dulbecco's Modified Eagle's Medium (DMEM) containing phenol red (Invitrogen), supplemented with the addition of 10 percent fetal bovine serum (FBS) (Hyclone), 100 IU/ml penicillin, 100 ug/ml streptomycin and 10 ug/ml ciprofloxacin hydrochloride.

Mouse-derived mesenchymal stem cells (MSCs) were cultured at 37 degrees Celsius and 5 percent Carbon Dioxide in Iscove's Modified Dulbecco Minimum Essential Medium (IDMEM) containing phenol red (Invitrogen), supplemented with the addition of 10 percent fetal bovine serum (FBS) (Hyclone), 10 percent horse serum (Hyclone), 100 IU/ml penicillin, 100 ug/ml streptomycin and 10 ug/ml ciprofloxacin hydrochloride.

Preparation of Extracellular Vesicle-Depleted Media.

To prepare extracellular vesicle-depleted (EV-depleted) media, FBS (Hyclone) was diluted 1:4 with base DMEM (Invitrogen) and was centrifuged at 100,000*g* for 17 hours at 4 degrees Celsius. The supernatant from these tubes was carefully removed top down by pipette, making sure to leave the bottom of the tube undisturbed. The supernatant was then filtered through a 0.22 µm filter (Millex) prior to being added to the base DMEM. The EV-depleted

media was then supplemented with 100 IU/ml penicillin, 100 ug/ml streptomycin and 10 ug/ml ciprofloxacin hydrochloride. EV-depleted IDMEM was prepared in the same manner as above, with the horse serum (Hyclone) also being diluted 1:4 with base media.

Transient Transfection of S15-GFP and miR-21 Constructs.

293T cells were transfected at approximately 60 percent confluency using Polyethylenimine (PEI), with equal parts miR-21 and S15-GFP plasmids. Media was changed to EV-depleted media 16 hours post-transfection, and supernatant was collected at 48, 72 and 96 hours post-transfection.

Extracellular Vesicle Collection and Concentration.

Supernatant collected from transiently transfected 293T cells was pooled and vesicles were isolated at 4 degrees Celsius by differential ultracentrifugation. Supernatant was spun at 4,000*g* for 20 minutes, 10,000*g* for 30 minutes, and 100,000*g* for 70 minutes. Vesicles were then concentrated by re-suspending the pelleted EVs in PBS and spun at 100,000*g* for another 70 minutes. These concentrated vesicle pellets were re-suspended in 500-1000 ul of PBS, transferred to fresh tubes, and stored at -20 degrees Celsius, if not used immediately.

MSC cells were plated, media changed to EV-depleted media the following day, and supernatant was collected at 24, 48 and 72 hours after the initial media change. Collected supernatant was pooled and vesicles were isolated and concentrated in the same manner as described above.

Molecular Beacon Experiments and Immunofluorescent Staining.

The molecular beacon targeting miR-21 used in these studies was the following:

5’-Cy3-GCGCGTCAACATCAGTCTGATAAGCTACGCGC-BHQ2-3’ (IDT). Concentrated extracellular vesicles collected from S15-GFP expressing 293T cells were mixed in PBS with the molecular beacon and either 0.2 U/ml Tris(2-carboxyethyl)phosphine hydrochloride (TCEP) (Sigma)-activated Streptolysin O (SLO) (Sigma), 0.01 percent saponin, or 0.01 percent digitonin, or were not mixed with any detergent. These mixtures were then spinoculated onto glass coverslips at 13 degrees Celsius for 2 hours at 1200*g* and subsequently fixed with a solution consisting of 0.1M PIPES and 3.7 percent formaldehyde (Polysciences) for 10 minutes.

Concentrated extracellular vesicles collected from MSC cells were mixed in PBS with the the molecular beacon and either 0.2 U/ml TCEP-activated SLO or were not mixed with a detergent. The mixtures were spinoculated and fixed in the same manner as described above. Following fixation, the EVs were incubated with one of two primary antibodies: mouse anti-CD81 (BD Pharmigen, 1:1000) or mouse anti-CD63 (BD Pharmigen, 1:1000), in a PBS block solution supplemented with 10 percent normal donkey serum (NDS), and 0.01 percent NaN3 for 1 hour. The EVs were then incubated with secondary antibody conjugated to a fluorophore, donkey anti-mouse 488 (Jackson ImmunoResearch), at a concentration of 1:400 in the same PBS block solution for 20 minutes.

Wide-Field Deconvolution Microscopy and Analysis.

Extracellular vesicles were imaged on a DeltaVision wide field fluorescent microscope (Applied Precision, GE) outfitted with a digital camera (CoolSNAP HQ; Photometrics), using a 1.4 numerical aperture, and 60 X objective lens. The acquired images were deconvolved with the SoftWoRx deconvolution software (Applied Precision) and analyzed on Bitplane: Imaris software version 7.6.4.

Puncta in the images were analyzed for size and sphericity, and separate surface algorithms were built around the GFP and Cy3 signals. These two algorithms were applied to all acquired images via the Batch Coordinator tool (Bitplane). The maximum fluorescence intensity found within each of these surfaces was then analyzed and cross analyzed with the other channel. All statistical analyses and graphs were created using GraphPad Prism version 6.00 (GraphPad Software, Inc.).

Differentiation of the Biogenesis Pathways of Extracellular Vesicles Containing HIV-1 Proteins Relevant to HAND through Drug Manipulation of Autophagy

Cell Culture.

HEK293T (293T) cells and human microglial clone C20 (C20) cells, a gift from the Karn laboratory (Case Western Reserve University), were cultured at 37 degrees Celsius and 5 percent Carbon Dioxide in Dulbecco's Modified Eagle's Medium (DMEM) containing phenol red (Invitrogen), supplemented with the addition of 10 percent fetal bovine serum (FBS) (Hyclone), 100 IU/ml penicillin, 100 ug/ml streptomycin and 10 ug/ml ciprofloxacin hydrochloride.

In preparation for EV experiments, C20 cells were transitioned to and thereafter cultured in the absence of FBS at 37 degrees Celsius and 5 percent Carbon Dioxide in DMEM containing phenol red (Invitrogen), supplemented with the addition of 10 percent Nu-Serum III (Corning), 100 IU/ml penicillin, 100 ug/ml streptomycin and 10 ug/ml ciprofloxacin hydrochloride.

Protein-GFP and Protein-Cherry Constructs.

Expression plasmids encoding HIV-1 proteins Tat, Nef, and Vpr fused to GFP had been previously generated by PCR-based strategy. Tat and Nef had been fused to the N-terminus of

GFP in a pEGFP-N1 backbone, and Vpr had been fused to the C-terminus of GFP in a pEGFP-C1 backbone. Tat-GFP had been previously subcloned into a lentiviral backbone, pLVX. Using PCR-based strategy, Nef-GFP was subcloned into the multiple cloning site of pLVX using the following oligonucleotide primer sequences:

FWD Nef 5'-GCTTCGAATTCGCCACCATGGGTGGCAAGTGGTCA-3'

REV GFP 5'-TAGGGCCCTTACTTGTACAGCTCGTCCATGCC-3'

GFP-Vpr was subcloned into a Tet inducible lentiviral backbone pLKO, a gift from the Bieniasz laboratory (Rockefeller University), using the following oligonucleotide primer sequences:

FWD GFP 5'-GGCCGAGAGGGCCGCCACCATGGTGAGCAAGGGCG-3'

REV Vpr 5'-GGCCAGAGAGGCCTTACTCTAGACTAGGATCTACT-3'

Fusion of Nef to the N-terminus of mCherry was generated by SOEing PCR strategy. Nef was amplified from Nef-GFP-pLVX, and mCherry was amplified from pLVX-mCherry-C1 using the following oligo nucleotide primers:

FWD Nef 5'-GCTTCGAATTCGCCACCATGGGTGGCAAGTGGTCA-3'

REV Nef 5’-CTTGCTGCTCCCCATGGTGGCGACCGGTGGATCCC-3'

FWD mCherry 5'-TCCACCGGTCGCCACCATGGGGAGCAGCAAGAGCA-3'

REV mCherry 5'-CCGGGCCCTTACTTGTACAGCTCGTCCATGCCGCC-3'

The resulting Nef-Cherry fusion was then subcloned into the multiple cloning site of pLVX.

Generation of Stable Tat-GFP and Nef-GFP C20 Cell Lines.

293T cells were transfected at approximately 70 percent confluency using Polyethylenimine (PEI), with equal parts of vesicular stomatitis virus glycoprotein (VSV-G), packaging construct psPax2, and Tat-GFP-pLVX or Nef-GFP-pLVX to obtain lentivirus for

transduction. Viruses were harvested 48 hours post-transfection, filtered through a 0.45-mm filter (Millipore), and used to transduce C20 cells. Due to the resistance of C20 cells to selection by puromycin, successfully transduced cells were selected by cell sorting for GFP+ cells using the FACSAria™ III (BD Biosciences).

Generation of Stable Tat-GFP Nef-Cherry C20 Cell Line.

293T cells were transfected at approximately 70 percent confluency using Polyethylenimine (PEI), with equal parts of vesicular stomatitis virus glycoprotein (VSV-G), packaging construct psPax2, and Nef-Cherry-pLVX to obtain lentivirus for transduction. Viruses were harvested 48 hours post-transfection, filtered through a 0.45-mm filter (Millipore), and used to transduce Tat-GFP C20 cells. Due to the resistance of C20 cells to selection by puromycin, successfully doubly transduced cells were selected by cell sorting for GFP+mCherry+ cells using the FACSAria™ III (BD Biosciences).

Generation of Doxycycline-Inducible GFP-Vpr C20 Cell Line.

293T cells were transfected at approximately 70 percent confluency using Polyethylenimine (PEI), with equal parts of vesicular stomatitis virus glycoprotein (VSV-G), packaging construct psPax2, and GFP-Vpr-pLKO to obtain lentivirus for transduction. Viruses were harvested 48 hours post-transfection, filtered through a 0.45-mm filter (Millipore), and used to transduce C20 cells. 48 hours post-transduction, cells were put under selection in DMEM containing 10 ug/mL blasticidin.

In order to confirm this inducible system was functional, cells were plated on fibronectin-coated coverslips in a 24-well plate at density of ~100,000 cells and treated overnight with 500 ng/mL doxycycline. Cells were fixed the following morning with a solution

consisting of 0.1 M PIPES and 3.7 percent formaldehyde (Polysciences) for 20 minutes and incubated with Hoechst in a PBS block solution supplemented with 10 percent normal donkey serum (NDS), 0.01 percent NaN3, and 0.1% saponin for 30 minutes. Cells were imaged on a DeltaVision wide field fluorescent microscope (Applied Precision, GE) outfitted with a digital camera (CoolSNAP HQ; Photometrics), using a 1.4 numerical aperture, and 60 X objective lens. The acquired images were deconvolved with the SoftWoRx deconvolution software (Applied Precision) and analyzed on Bitplane: Imaris software version 7.6.4.

Drug Manipulation of Autophagy to Alter Extracellular Vesicle Flux.

In drug manipulation of autophagy, C20 cells were treated overnight with 100 nM bafilomycin A1 or DMSO vehicle control. Alternatively, C20 cells were treated overnight with 100nM rapamycin in combination with starvation by culturing in base DMEM without Nu-Serum III supplementation. For GFP-Vpr C20 cells, all of these treatments were performed in the presence of 500ng/mL doxycycline to induce the expression of GFP-Vpr. Supernatant was collected the following day, and was spun at 10,000*g* for 30 minutes to remove cells and cellular debris. If not used immediately for an experiment, the supernatant was covered in foil to prevent photobleaching and stored at 4 degrees Celsius.

Immunofluorescent Staining.

Collected supernatant was spinoculated onto glass coverslips at 13 degrees Celsius for 2 hours at 1200*g* and subsequently fixed with a solution consisting of 0.1 M PIPES and 3.7 percent formaldehyde (Polysciences) for 10 minutes. Following fixation, the EVs collected from TatGFP or NefGFP cell lines were incubated with mouse anti-CD63 (BD Biosciences, 1:1000) and either rabbit anti-LAMP1 (Abcam, 1:1000) or rabbit anti-p62 (Cell Signaling Technology, 1:1000), in a

PBS block solution supplemented with 10 percent NDS, and 0.01 percent NaN3 for 1 hour. The EVs were then incubated with secondary antibodies conjugated to fluorophores, donkey anti-mouse Alexa 647 and donkey anti-rabbit Alexa 594 (both Jackson ImmunoResearch), at a concentration of 1:400 in the same PBS block solution described above for 20 minutes. For EVs collected from the TatGFPNefCherry cell line, EVs were incubated with either mouse-antiCD63 (BD Biosciences, 1:1000) or rabbit anti-LAMP1 (Abcam, 1:1000) for 1 hour in the block described above, followed by a 20 minute incubation with secondary antibodies conjugated to fluorophores, either donkey anti-mouse Alexa 647 or donkey anti-rabbit Alexa 647, in the block described above.

Wide-Field Deconvolution Microscopy and Analysis.

Extracellular vesicles were imaged on a DeltaVision wide field fluorescent microscope (Applied Precision, GE) outfitted with a digital camera (CoolSNAP HQ; Photometrics), using a 1.4 numerical aperture, and 60 X objective lens. The acquired images were deconvolved with the SoftWoRx deconvolution software (Applied Precision) and analyzed on Bitplane: Imaris software version 7.6.4.

Puncta in the images were analyzed for size and sphericity, and separate surface algorithms were built around the GFP, Alexa 594, Alexa 647, and mCherry signals. These algorithms were applied to all pertinent acquired images via the Batch Coordinator tool (Bitplane). The maximum fluorescence intensity found within each of these surfaces was then analyzed and cross-analyzed with the other channels. All statistical analyses and graphs were created using GraphPad Prism version 6.00 (GraphPad Software, Inc.).

Western Blotting and Western Antibodies.

Whole cell lysates were prepared by lysing pelleted cells in a buffer composed of 100mM Tris pH 8.0, 1% NP- 40, and 150 mM NaCl and a protease inhibitor cocktail (Roche) for 30 minutes on ice. After lysis, samples were centrifuged at 14,800*g* for 10 minutes and the supernatants collected. The protein concentration of the supernatants was measured by the Pierce BCA protein assay kit (Thermo Scientific). Samples were mixed with Laemmli 2× SDS sample buffer and boiled for 5 min, and equal amounts of protein were loaded on a 10 percent polyacrylamide gel for SDS-polyacrylamide gel electrophoresis (SDS-PAGE). After separation, proteins were transferred onto nitrocellulose membranes (Bio-Rad) and incubated with primary antibodies, either rabbit anti-green fluorescent protein (GFP) (Santa Cruz, 1:1000) or rabbit anti-mCherry (BioVision, 1:1000), overnight in powdered milk block solution 2.5g/50mL TBST. Following washing, the nitrocellulose membranes were incubated with anti-rabbit secondary conjugated to Horseradish Peroxidase (HRP) (Thermo Scientific, 1:10000). HRP-conjugated antibodies were then detected using SuperSignal West Femto Chemiluminescent Substrate (Thermo Scientific) and the chemiluminescence levels analyzed with the FlourchemE Imaging System (Protein Simple).

CHAPTER FOUR

DETECTION OF MICRORNAS IN INDIVIDUAL EXTRACELLULAR VESICLES WITH A MOLECULAR BEACON

Introduction

Both virally-derived miRNAs and deregulated host miRNAs that are packaged into EVs have been implicated in HAND pathogenesis.[10,11,13,14] One of the struggles when it comes to the study of EVs is that the majority of techniques used to look at their characteristics, such as chemical composition, cannot resolve individual EVs from one another. Such techniques are useful in studying EVs as a whole, but these bulk studies cannot get down to the level of minute details to differentiate between the many subpopulations within these highly heterogenous mixtures. The ability to hone in on these specifics could give a better understanding in the highly complex dynamics of EV biogenesis, the targeting of specific cargo to specific EVs, and the functional bioactivity of specific EV populations. Previously in our laboratory, we have combined techniques used in the study of viruses with wide-field deconvolution fluorescence microscopy to begin to study EVs at a single vesicle level. While techniques like Nanoparticle Tracking Analysis (NTA) measure individual EVs based on Brownian motion, laser channel limitations combined with issues of rapid photobleaching, altered motion due to bound antibodies, and self-association of lipophilic dyes into EV-like nanoparticles make fixed-imaging the better technique for our fluorescence-based detection of multiple EV cargoes. With the use of Bitplane Imaris imaging software we are able to build algorithms to create surface masks

around individual EV puncta based on a variety of characteristics, such as size and sphericity (Figure 2C). By applying these algorithms to all the images we acquire in an experiment, we can assess the individual qualities of thousands of these surfaces simultaneously. Being a fluorescence-based technique, the primary aspect each surface is surveyed for is the intensity of a fluorescent signal. When using multiple fluorescent signals, each surface can be assessed for the intensities of each signal, providing valuable information on the co-localization of two signals, which in turn provides insight into the distribution of specific proteins or other components that these fluorescent signals correspond to in these various EV populations (Figure 2E). Thus far, we have used this technique with fluorescently-tagged fusion proteins and the immunofluorescent labelling of proteins. Successful adaptation of this system to evaluate the RNA or miRNA content of individual EVs would create a powerful tool in further understanding the differences in EV populations in general, but also in understanding their roles in HAND.

Experimental Design

To assess the use of a fluorescently-tagged molecular probe as a valid approach to survey the miRNA content of individual EVs in the context of our single vesicle analysis method, I chose to use a molecular beacon. Molecular beacons are synthetic DNA constructs that contain a probe region complementary to the target sequence, which is flanked by short sequences that are complementary to each other that in turn forms their characteristic stem-loop structure.[101] These probes are dually tagged, with one end of the construct connected to a fluorophore and the other end connected to a quencher dye. When the target sequence is not present the stem-loop structure is maintained, keeping the fluorophore and quencher in close

proximity and consequently preventing a fluorescent signal.[101] When the target sequence is present, the probe region hybridizes to it, linearizing the molecular beacon structure in the process and separating the fluorophore from the quencher, allowing a fluorescent signal.[101]

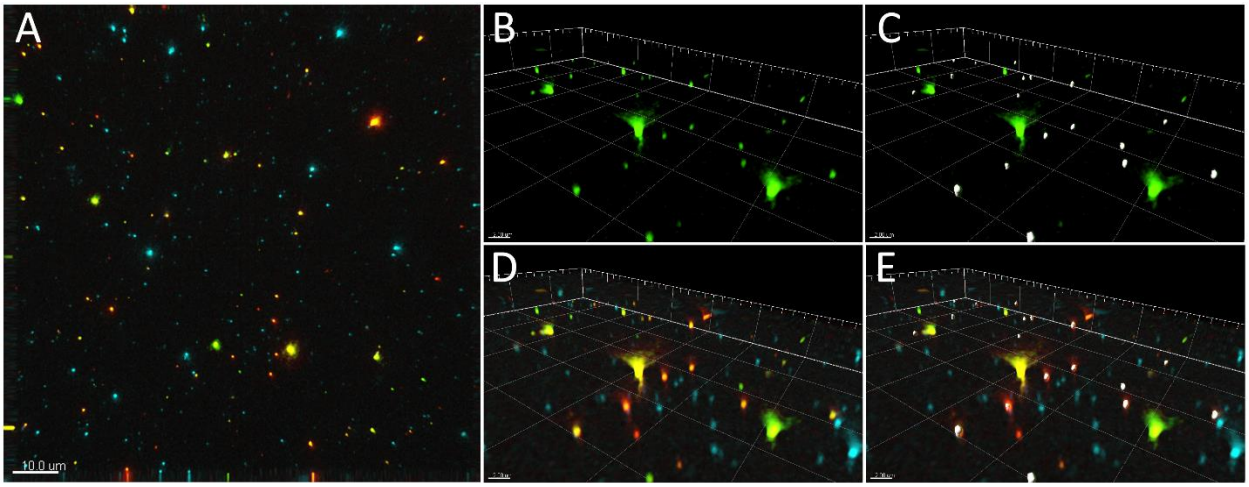

Figure 2. Single Vesicle Analysis Method. Representative images of our fluorescence-based single vesicle analysis method. **(A)** Full image with all three channels. **(B)** Zoomed in, showing FITC channel only. **(C)** Algorithm applied to create surface masks for the FITC channel. **(D)** Zoomed in, showing all channels. **(E)** FITC channel surface masks applied. Within these FITC surface masks, the intensity of the other channels can be assessed, and co-localization of the signals can be determined.

The beacon I chose to use is this Cy3-labelled molecular beacon specific for human microRNA 21 (miR-21): 5'-Cy3-GCGCGTCAACATCAGTCTGATAAGCTACGCGC-BHQ2-3'.[102] Previously published by Lee et al. in 2015, this molecular beacon was validated as a method to assess the miR-21 content of EVs, as a high amount of signal was only observed when incubated with EVs collected from a breast cancer cell line that highly expresses miR-21 and was not observed when incubated with EVs from a cell line that does not express miR-21.[102] However, like many other methods in EV studies, this study looked at EVs as a whole, using a plate reader to assess the total fluorescence of this whole EV population.[102] I hoped to incorporate the use of this molecular beacon into our single vesicle analysis method to detect miR-21 in individual EVs.

An important note, our lab supplements media with fetal bovine serum (FBS). EVs are commonly found in and can be isolated from human serum, and FBS is no exception. To reduce the amount of FBS-derived EVs potentially contaminating my experiments, all experiments were performed in media that had been depleted of EVs by ultracentrifugation and filtration of the FBS prior to its addition to the media.

Initial Experiments with Overexpression of miR-21.

A common marker used in virion and EV studies is a fusion of the first 15 residues of a Src kinase with a fluorescent protein.[103] This N-terminal region of Src becomes post-translationally modified by the addition of a myristoyl group. This myristoylation allows Src to associate with lipid membranes, and this can be exploited to label virions and EVs, as fusion of this myristoylated domain to a fluorescent protein allows the fluorescent protein to associate with lipid membranes and become incorporated into budding virions and EVs.[103] In these studies, a fusion of this 15-residue portion of Src with green fluorescent protein (S15-GFP) was used as a marker for EVs. With the Cy3-labelled molecular beacon, I hoped to see co-localization of the Cy3 signal with the S15-GFP signal, indicating detection of miR-21 in an EV.

For initial experiments, human embryonic kidney 293T (HEK293T, or simply 293T) cells were transiently transfected with two overexpression vectors, one containing S15-GFP and the other containing human miR-21. Supernatant was collected from these cells and EVs were isolated and concentrated by differential ultracentrifugation. While there are many different methods in the field to isolate EVs from supernatant and serum, each with their own advantages and limitations, differential ultracentrifugation is still considered the “gold standard” and so is the method that was chosen for these studies.[104] Concentrated EVs were

then mixed with the Cy3-labelled miR-21 molecular beacon and different detergents, with the thought that permeabilization of the EVs would allow the beacon access to the luminal miRNAs and improve the amount of signal. These mixtures were spinoculated onto coverslips, imaged and analyzed by wide-field deconvolution microscopy.

Testing the Beacon in a miR-21 Knockout System.

As the previous experiments were in an overexpression system, the following experiments investigated the use of this molecular beacon at a more physiologically relevant level of expression, as well as in a system in which the target of the beacon had been knocked out. The cells of choice in these experiments were mouse mesenchymal stem cells (MSCs). MSCs are multipotent stem cells with the capacity to differentiate into a variety of stromal cell types and miR-21 appears to be a critical factor involved in their differentiation into these different cell types.[105] Mouse bone marrow-derived wild type (WT) MSCs and a stable miR-21 knockout (KO) line of these cells were provided by the Jones laboratory (Loyola University Chicago). Since these are mouse-derived MSCs and the molecular beacon targets human miR-21, the sequences of miR-21 from both species were aligned to ensure there were no major differences and the beacon would still bind to the mouse homolog (Figure 3).

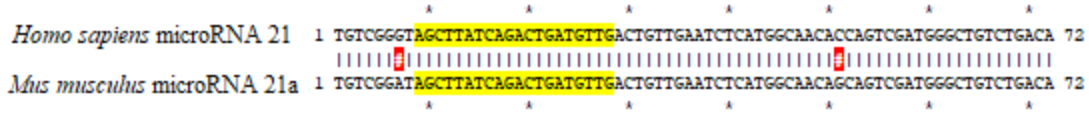

Figure 3. Alignment of human and mouse miR-21 genes. Alignment of human miR-21 (top sequence) and mouse miR-21a (bottom sequence) showed two mismatched base pairs between the two sequences, but neither are in the region of the fully processed miRNA to which the molecular beacon is complementary and binds (highlighted in yellow).

Experiments were carried out in a similar manner as before, with the collection of supernatant from these cells and subsequent isolation and concentration of EVs by differential ultracentrifugation. Concentrated EVs were mixed with the Cy3-labelled miR-21 molecular beacon in the presence or absence of a detergent and spinoculated onto coverslips. As these WT and miR-21 KO MSCs were not expressing any fluorescent proteins to serve as EV markers, EVs were immunostained for common EV markers CD63 and CD81, followed by secondaries conjugated to Alexa Fluor 488. An important note, the primary antibodies used in these studies were raised in mouse against the human versions of CD63 and CD81. While these proteins are highly conserved across species, there are potentially slight differences in the three-dimensional structures of these proteins between mouse and human. As a highly ubiquitous protein, production of antibodies against highly conserved or mouse-specific epitopes would be lethal to the mouse host, and the antibodies that get selected for are thus likely against human-specific epitopes. With the MSCs being mouse-derived and therefore expressing mouse CD63 and CD81, the human-specificity of these antibodies could potentially affect our results. After immunostaining, the coverslips were imaged and analyzed by wide-field deconvolution microscopy.

Results

Initial Experiments with Overexpression of miR-21.

Results of the overexpression experiments in 293T cells were unexpected. The S15-GFP and the Cy3-labelled miR-21 molecular beacon signals rarely co-localized (Fig 4C). Additionally, permeabilization with detergents did not appear to be necessary as it neither enhanced co-localization nor increased the total number of Cy3 puncta. In fact, the greatest amount of S15-

GFP positive puncta and the greatest amount of Cy3 positive puncta were seen in the absence of a detergent, with permeabilization appearing to decrease our overall amount of either signal (Fig 5). This was most drastically observed with saponin and digitonin treated samples, which virtually eliminated the S15-GFP signal and decreased the amount of Cy3 signal by about 4-fold compared to samples not treated with a detergent.

Testing the Beacon in a miR-21 Knockout System.

In this system, I anticipated less Cy3 beacon signal in EVs isolated from the WT MSCs than in the 293T experiments, given that the miR-21 is expressed at normal levels for the cell type instead of being grossly overexpressed by an expression vector. With the EVs collected from miR-21 KO MSCs, I expected no or background levels of beacon signal. Since S15-GFP in the previous experiments did not co-localize with the beacon signal, the hope was that using more canonical EV markers such as CD63 and CD81, would result in some level of co-localization to indicate miR-21 was being detected within an EV. However, the attempts at immunostaining against these EV markers were largely unsuccessful, with little to EVs staining positive for CD63 or CD81. This complicated the analysis, as no co-localization data could be examined to validate that the beacon could detect miR-21 inside of an EV. Additionally, the molecular beacon signal that was detected did not appear to differ between WT and miR-21 KO samples (Figure 6).

Conclusions

The goal of this study was to develop a method to detect miRNA content of EVs at a single vesicle level through the use of a molecular beacon probe. This was, unfortunately, not achieved. While beacon signal was detected among isolated EVs collected from miR-21

overexpressing 293T cells, the signal did not co-localize with the S15-GFP EV marker. It is possible that miR-21 is simply packaged into an entirely separate population of EVs than the ones S15-GFP are incorporated into. Regrettably, this was not explored any further as the unsuccessful immunostaining against CD63 and CD81 in the MSC experiments provided no salvageable EV marker data. The presence of the beacon signal in the miR-21 KO samples is concerning and may suggest the beacon is binding non-specifically. However, it is also important to consider that this apparent non-specific signal may be the result of the beacon becoming linearized too easily, as its hairpin structure is held together by a mere 6 base pairs. Overall, it is clear that a lot of optimizing will need to be done in order to further assess if this molecular beacon can be incorporated into our single vesicle analysis method to accurately assess the miRNA content of a single EV. The beacon should have been assessed with more stringent control experiments to determine the specificity of the signal, perhaps through testing of the beacon in cells which would contain a much higher concentration of miR-21 than individual EVs.

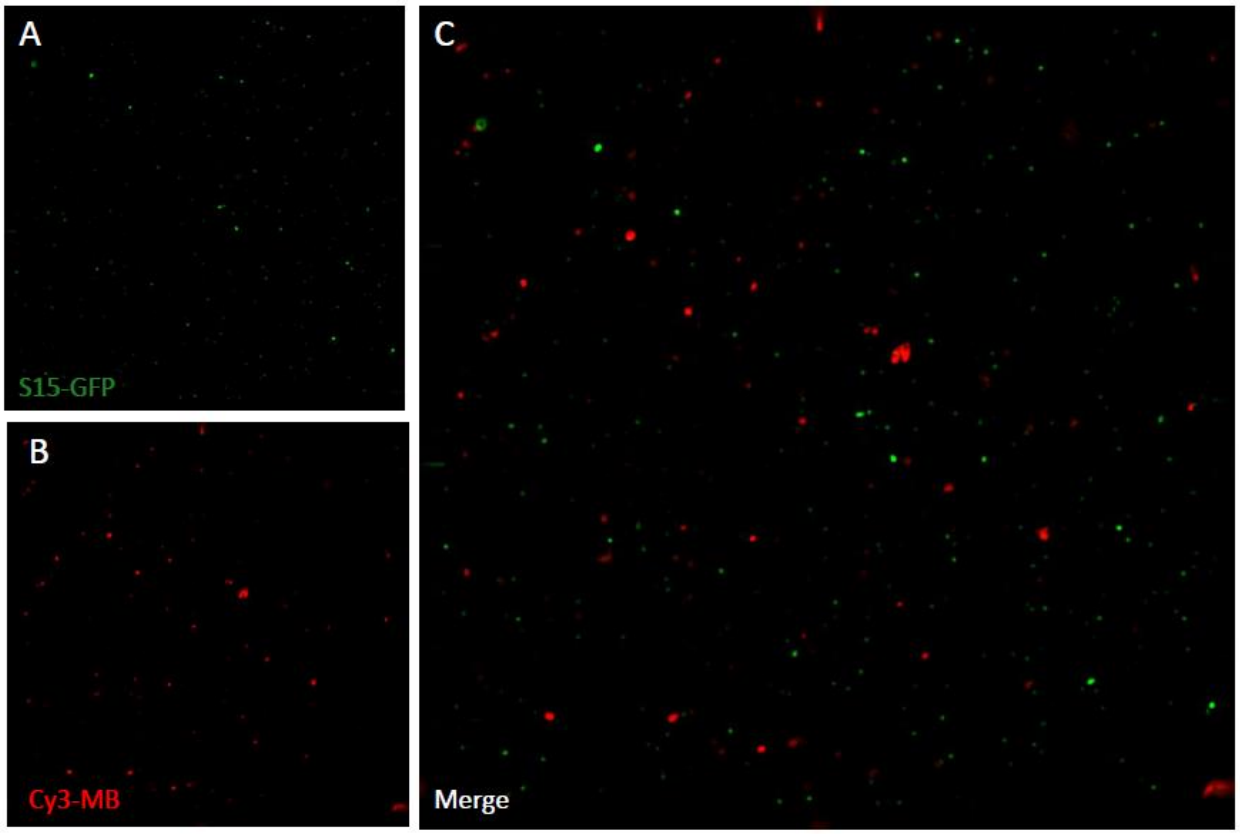

Figure 4. Representative Image of Molecular Beacon Experiments. Concentrated EVs collected from S15-GFP 293Ts overexpressing miR-21 were mixed with the miR-21 molecular beacon. **(A)** Green FITC channel only showing the S15-GFP signal. **(B)** Red channel only showing the Cy3 molecular beacon signal. **(C)** The two channels merged. Note the lack of yellow puncta that would indicate co-localization of these two signals.

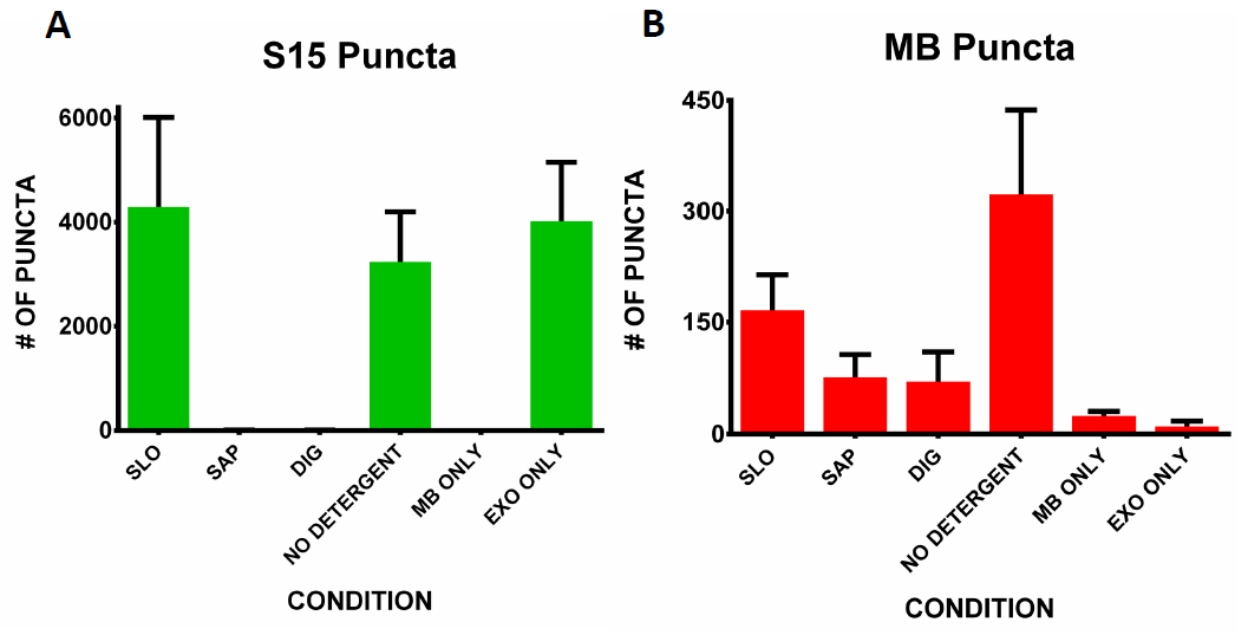

Figure 5. S15-GFP 293T Molecular Beacon Experiments. (A) Total S15GFP+ puncta. **(B)** Total Cy3+ molecular beacon puncta. This data is the summation of three replicates, with the error bars showing the standard error of the mean.

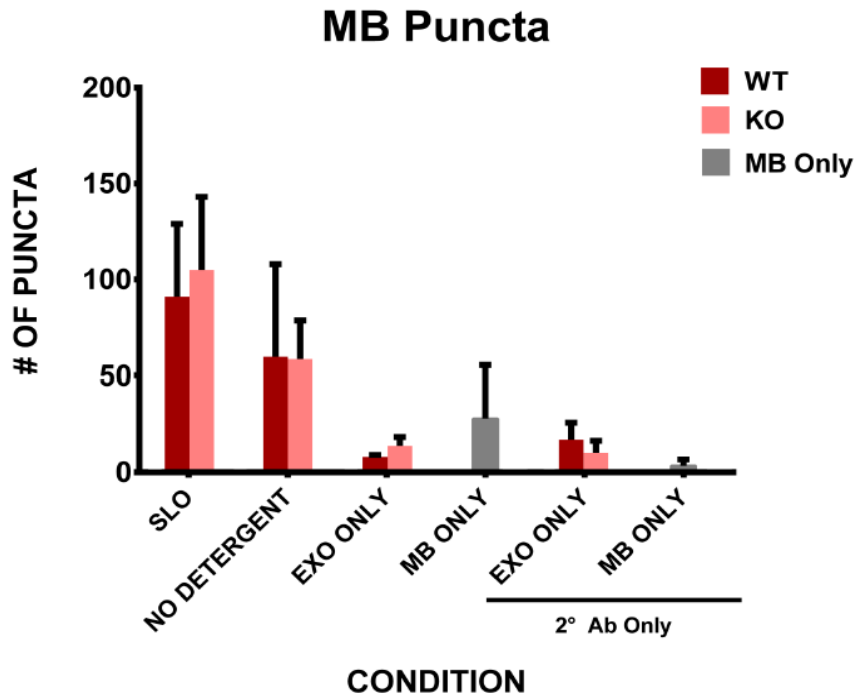

Figure 6. MSC Molecular Beacon Experiments. Total Cy3+ molecular beacon puncta in experiments using EVs isolated from MSCs. This data is the summation of three replicates, with the error bars showing the standard error of the mean.

CHAPTER FIVE

DIFFERENTIATION OF THE BIOGENESIS PATHWAYS OF EXTRACELLULAR VESICLES CONTAINING HIV-1 PROTEINS RELEVANT TO HAND THROUGH DRUG MANIPULATION OF AUTOPHAGY

Introduction

HIV-1 proteins Tat, Nef, and Vpr are among the many pathogenic components of HIV-1 that appear to contribute to the neuropathology that leads to the symptoms of HAND. Their incorporation into EVs and subsequent transfer to other cells, particularly neurons, is thought to account for the wide-spread pathology observed in the brain of HIV-1 patients, as active HIV-1 replication in the brain is very localized.[5,12,26] Previous work in our lab began to look at the EV markers these proteins associated with and found that Tat often co-localized with LAMP1, Nef often co-localized with CD9 and CD81, and Vpr often co-localized with TSG101. Based on these markers, some inferences were made about the biogenesis of these EV populations that contained these different HIV-1 proteins.

Lysosomal-associated membrane protein 1 (LAMP1), as its name suggests, is a transmembrane protein found to be enriched in the membrane of lysosomes. LAMP1 and its close relative LAMP2 have both been found to be essential in lysosome biogenesis and the proper function of autophagy.[106,107] As such, LAMP1 was used as a marker for the unconventional autophagic EV secretion pathway in our studies. This choice was supported by a recent study looking at the unconventional secretion of α-synuclein that reported LAMP2 to be enriched in EVs upon alteration of autophagy with bafilomycin A1.[99] With Tat's known ability to

mess with cellular membranes and alter autophagy in cells,[15,50] the high co-localization of Tat with LAMP1 in EVs was taken as a hint that Tat-containing EVs were derived from this unconventional autophagic secretion pathway.

CD9 and CD81 are two of the tetraspanins commonly complexed together and found on the cell surface, with their cytoplasmic domains typically interacting with various molecules important in cell signaling cascades, as well as elements of the cytoskeleton.[67] With apparent roles in EV biogenesis, they are commonly found in EVs and are used as common EV markers.[52,67] Much like Src kinase, the N-terminus of Nef is myristoylated, allowing it to associate to cellular membranes. With the combination of this ability to associate with membranes and the high co-localization with CD9 and CD81, Nef-containing EVs were suspected to bud directly from the plasma membrane.

Tumor susceptibility gene 101 (TSG101) is a component of the ESCRT-I complex involved in endosomal cargo sorting and inward budding of ILVs in the process of MVB formation.[52] TSG101 has long been known to be involved in the budding and release of new virions during HIV-1 infection, and recent studies have found that Vpr interacts with TSG101 in tandem with another viral protein, Gag.[108] Gag has been shown to be involved in the recruitment of TSG101 to the plasma membrane to facilitate virion budding.[108] Due to the high co-localization of Vpr with TSG101 in EVs in the absence of Gag expression, and thus the lack of recruitment of TSG101 to the plasma membrane, Vpr-containing EVs potentially arise from the classical exosome biogenesis pathway and are released when a MVB fuses with the plasma membrane.

Experimental Design

As our previous studies of Tat, Nef, and Vpr EVs were done primarily through the transient transfection of fluorescently-tagged fusions of these proteins in 293T cells, I strived to improve the physiological relevancy of our characterization of these EVs. To achieve both a more relevant level of expression and more relevant cell type, lentiviral constructs containing the fluorescent fusion proteins were transduced into human microglial clone 20 (C20) cells. Briefly, fusions of the viral proteins to GFP or mCherry were created by PCR-based strategies, subcloned into lentiviral vectors (Supplemental Figure 1A-C) and transduced into C20 cells. Because Vpr induces cell cycle arrest and apoptosis, a special Tet-inducible lentiviral vector was used to express it in C20 cells (Supplemental Figure 1D-E). In an additional attempt to improve physiological relevancy, Tat-GFP and Nef-mCherry were co-expressed in C20 cells.

Another change between these and previous studies is the use of a serum replacement over FBS supplementation in media. By using a serum alternative, I eliminated the possibility of FBS-derived EV contamination in my studies.

Manipulation of Unconventional Autophagic EV Secretion.

With Tat's high degree of co-localization with LAMP1 in EVs and the recent indication that LAMP proteins are enriched in EVs upon alteration of autophagy,[99] the unconventional autophagic secretion pathway seemed like the perfect EV biogenesis pathway to focus on first. Additionally, autophagy is vital for the proper function of terminally-differentiated cells such as neurons, and the dysregulation of autophagy in neurons and other cells of the brain by HIV-1 components (Tat in particular) likely contributes to the pathology of HAND.[92] I used two drugs to alter the autophagic flux in cells: rapamycin and bafilomycin A1.

An antibiotic produced by *Streptomyces hygroscopicus*, rapamycin inhibits mTOR, a kinase in mammalian cells that suppresses autophagy.[96] By inhibiting mTOR, rapamycin stimulates autophagy, particularly when combined with serum starvation. Since the cells in these experiments were cultured in the absence of actual serum, the same effect was achieved by culturing cells in base medium without that supplementation of the serum replacement. While overstimulation of autophagy in this manner increases the degradation of many proteins, this overstimulation could also potentially overwhelm the cell and result in increased unconventional autophagic secretion.[96]

Bafilomycin A1 is an antibiotic produced by *Streptomyces griseus* that prevents lysosome acidification, which in turns leads to impaired fusion of lysosomes with autophagosomes.[96] As such, bafilomycin A1 is considered an autophagy inhibitor as it inhibits the final stages of autophagy, in which the degradation of the contents of the autophagosome occurs. Consequently, bafilomycin A1 leads to the accumulation of autophagosomes in cells, which results in increased unconventional autophagic secretion as these blockaded autophagosomes are redirected to fuse with the plasma membrane.[96]

In altering autophagic flux with these treatments, I expected to see differences between the HIV-1 protein EV populations. If the high co-localization of Tat with LAMP1 observed in previous studies indicates the biogenesis of Tat EVs by the unconventional autophagic secretion pathway, then the amount of Tat-GFP EVs released from both the Tat-GFP and TatGFP-NefCherry C20 cells will increase with stimulation of autophagy by rapamycin and the inhibition of the late degradative phase of autophagy by bafilomycin A1. If the high co-localization of Nef and Vpr with markers other than LAMP1 indicates that Nef and Vpr EVs do not arise from the

unconventional autophagic secretion pathway, then the amount of Nef-GFP/Cherry and GFP-Vpr EVs released from the Nef-GFP, TatGFP-NefCherry, and GFP-Vpr C20 cells, respectively, will not change upon alteration of autophagy by treatment with rapamycin or bafilomycin A1.

Cells were treated with 100nM rapamycin, 100nM bafilomycin A1, or a DMSO vehicle control (plus 500ng/mL doxycycline for the GFP-Vpr cells to induce its expression) overnight and supernatant collected the following morning. EVs were isolated by a modified version of the complete differential ultracentrifugation protocol, that removed cells and cellular debris but did not pellet and concentrate the EVs. EVs were then spinoculated onto to coverslips, and immunostained for combinations of the MVB EV marker CD63, and the autophagic markers LAMP1 and p62, followed by fluorescently-conjugated secondaries. Coverslips were imaged and analyzed by wide-field deconvolution microscopy.

Results

Manipulation of Unconventional Autophagic EV Secretion.

Despite cell imaging confirmation of the induction of GFP-Vpr in cells upon treatment with doxycycline (Supplementary Figure 1E), GFP-Vpr could not be detected during the imaging of EVs. Consequently, there is no data to report on GFP-Vpr EVs. Data was obtained for Tat-GFP and Nef-GFP/Cherry EVs, and the results are striking. Both Tat and Nef EVs increased upon rapamycin or bafilomycin A1 treatment, although the increase in Tat was consistently greater than the increase in Nef (Figure 7). My hypothesis that, based on previous marker co-localization data, Tat and Nef belonged to two distinct EV populations that arose from different biogenesis pathways implies that Tat and Nef would not be found in EVs together. However, when Tat-GFP and Nef-Cherry were expressed in the same cells, Tat and Nef frequently co-

localized (Figure 8A). Interestingly, the degree of co-localization depends on which surface channel is gated upon. Nef-Cherry positive surfaces were almost always Tat-GFP positive, while Tat-GFP positive surfaces were Nef-Cherry positive only less than half of the time (Figure 8A). These co-localizations remained relatively stable, not changing much with treatment of rapamycin or bafilomycin A1.

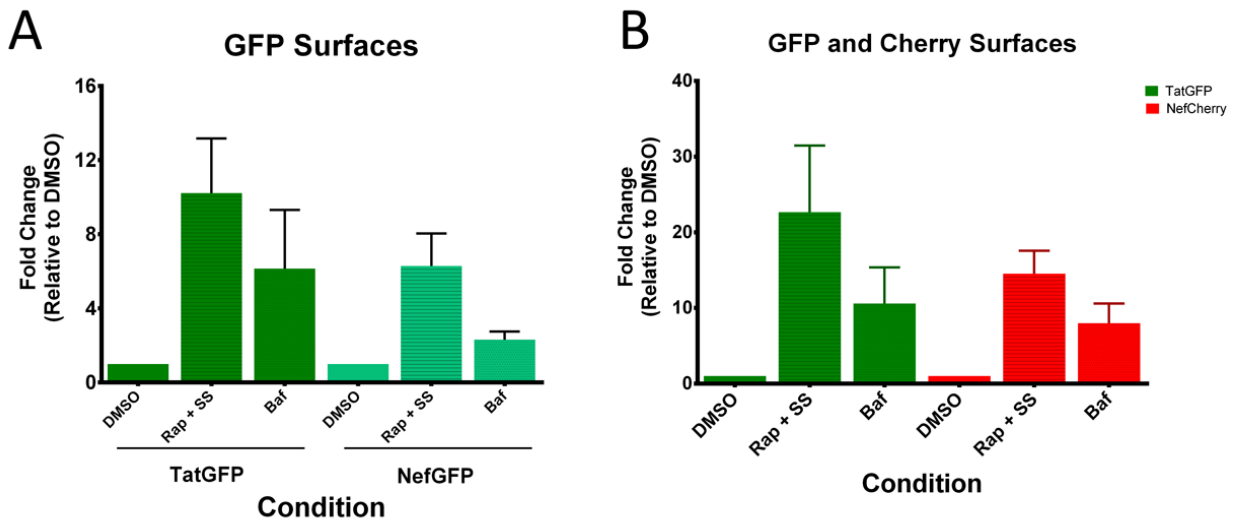

Figure 7. Fold Changes in Fusion Proteins. These graphs are the summation of three replicates and show the fold changes of Tat and Nef fusion proteins upon treatment with rapamycin and bafilomycin A1. Error bars report the standard error of the mean. **(A)** Changes in Tat-GFP and Nef-GFP. **(B)** Changes in Tat-GFP and Nef-Cherry.

Unlike previous observations that Tat highly co-localized with LAMP1, in these studies Tat-GFP co-localized with LAMP1 only a small percentage of the time in both the TatGFP-NefCherry (Figure 8C) and Tat-GFP alone cell lines (Figure 9B) and this amount of co-localization did not change with treatment of rapamycin or bafilomycin A1. Additionally, these co-localizations of Tat with LAMP1 are similar to the amount of co-localization of Nef with LAMP1, which was also minimal (Figure 8C and Figure 9B). Another marker of autophagic secretion, p62, was stained for in studies with Tat-GFP and Nef-GFP cells and, much like with LAMP1, co-

localization of Tat with p62 was low and comparable with Nef's co-localization with p62 (Figure 8C). Intriguingly, in untreated cells both Tat and Nef co-localized with the classical MVB marker CD63 40-60 percent of the time (Figure 8B and Figure 9A). Treatment with rapamycin or bafilomycin A1 consistently and drastically decreased the amount of CD63 co-localization of both Tat and Nef in Tat-GFP and Nef-GFP cells, respectively (Figure 9A). However, this reduction in CD63 co-localization was not observed when Tat and Nef where co-expressed in the TatGFP-NefCherry cells (Figure 8B).

It is extremely important to note that upon Western Blot evaluation of transduced C20 cells, the Tat and Nef fusion proteins were regularly cleaved (Figure 10). This was further evidenced by fluorescent imaging of transduced cells (data not shown) that found the GFP and mCherry signals to be more diffuse than punctate, unlike the images of induced GFP-Vpr (Supplementary Figure 1E) which by Western Blot analysis showed no cleavage product (Figure 10). This complicates analysis a great deal and brings into question whether any of the above observations were in fact "real". It is highly likely that free GFP and free mCherry were being incorporated into EVs instead of the fusion proteins, nullifying any inferences and conclusions concerning the biogenesis pathways of Tat-containing or Nef-containing EVs.

Unaffected by the cleavage products are the changes in the EV markers themselves (Figure 11). Treatment with either resulted in a slight increase in total EVs positive for LAMP1 or p62. Bafilomycin A1 increased the number of CD63 positive EVs, although not as strikingly so as rapamycin treatment.

Conclusions

The goal of this study was to attempt to differentiate the biogenesis pathways of EVs that contain different HIV-1 proteins. Previous studies had led to the hypothesis that Tat EVs were derived from the unconventional autophagic secretion pathway, and so this pathway was altered through drug manipulation of autophagy. Despite increases in Tat EVs resulting from these drug manipulations, increases (albeit slightly less) were also observed for Nef EVs which were hypothesized to bud directly from the plasma membrane and not the unconventional autophagic secretion pathway. Unexpectedly, Tat and Nef frequently co-localized when expressed in the same cells. And lastly, Tat co-localized with autophagic secretion markers LAMP1 and p62 only minimally. Together these data bring my initial assumptions into question. They potentially suggest Tat EVs and Nef EVs are not derived from separate pathways, and with the minimal of co-localization with LAMP1 and p62 it is unclear if either are being derived from the unconventional autophagic secretion pathway despite secretion of both clearly being altered by disruption of normal autophagy.

Ultimately, any conclusions that are drawn from these studies must be accepted with a great deal of caution. When expressed in C20 cells, the linker between these fusion proteins appears to get cleaved quite frequently so it is possible the fluorescent signals detected in these studies are not Tat-GFP, Nef-GFP, and Nef-Cherry, but free GFP and Cherry.

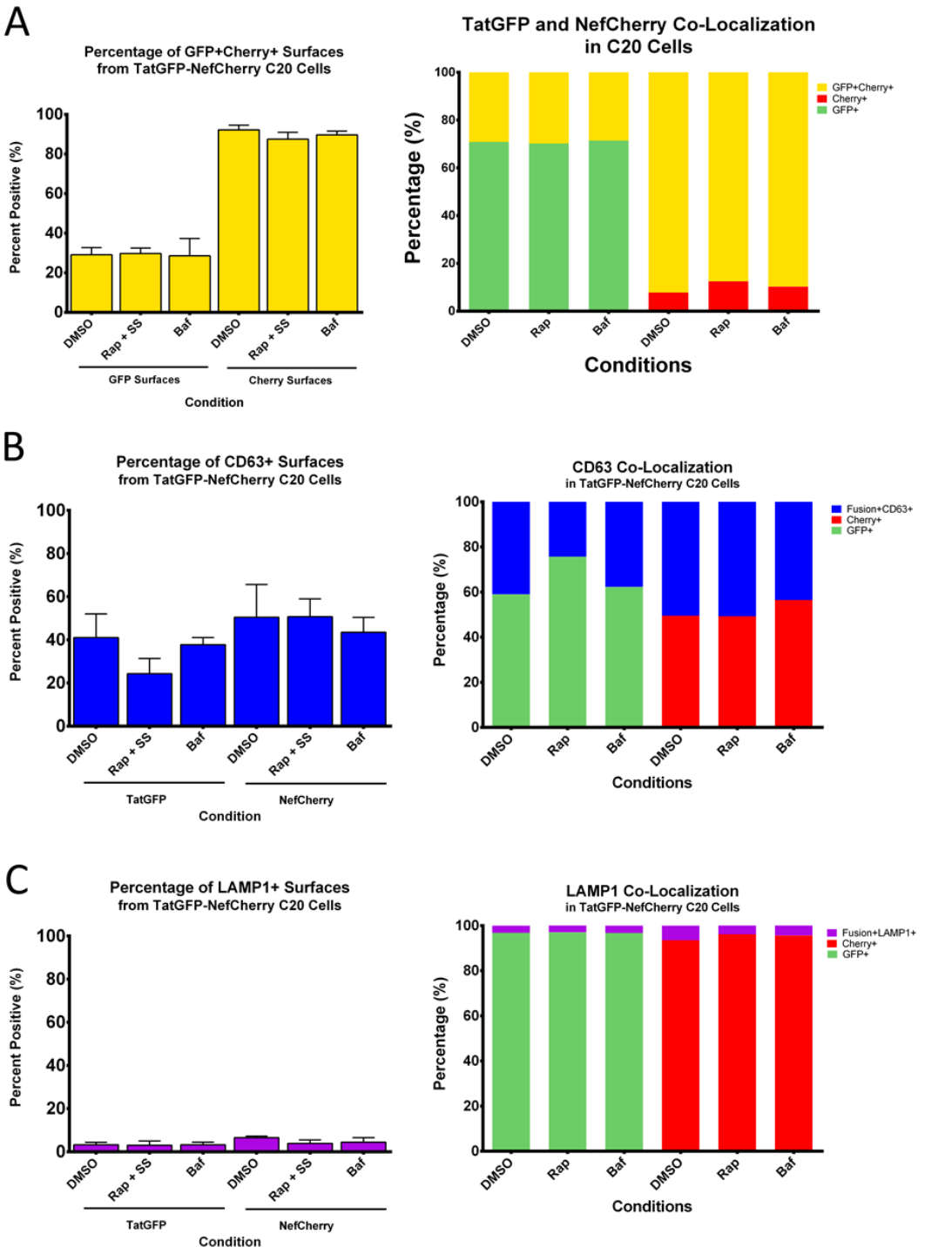

Figure 8. TatGFP-NefCherry C20 EV Co-Localization Data. The summation of co-localization data of three replicates, with the error bars showing the standard error of the mean. Graphs in the left-hand column show the percent positive surfaces for the marker of interest. Graphs in the right-hand column represent the summation of both the surfaces positive and negative for the marker of interest. **(A)** Co-localization of TatGFP and NefCherry together. **(B)** Co-localization with CD63. **(C)** Co-localization with LAMP1.

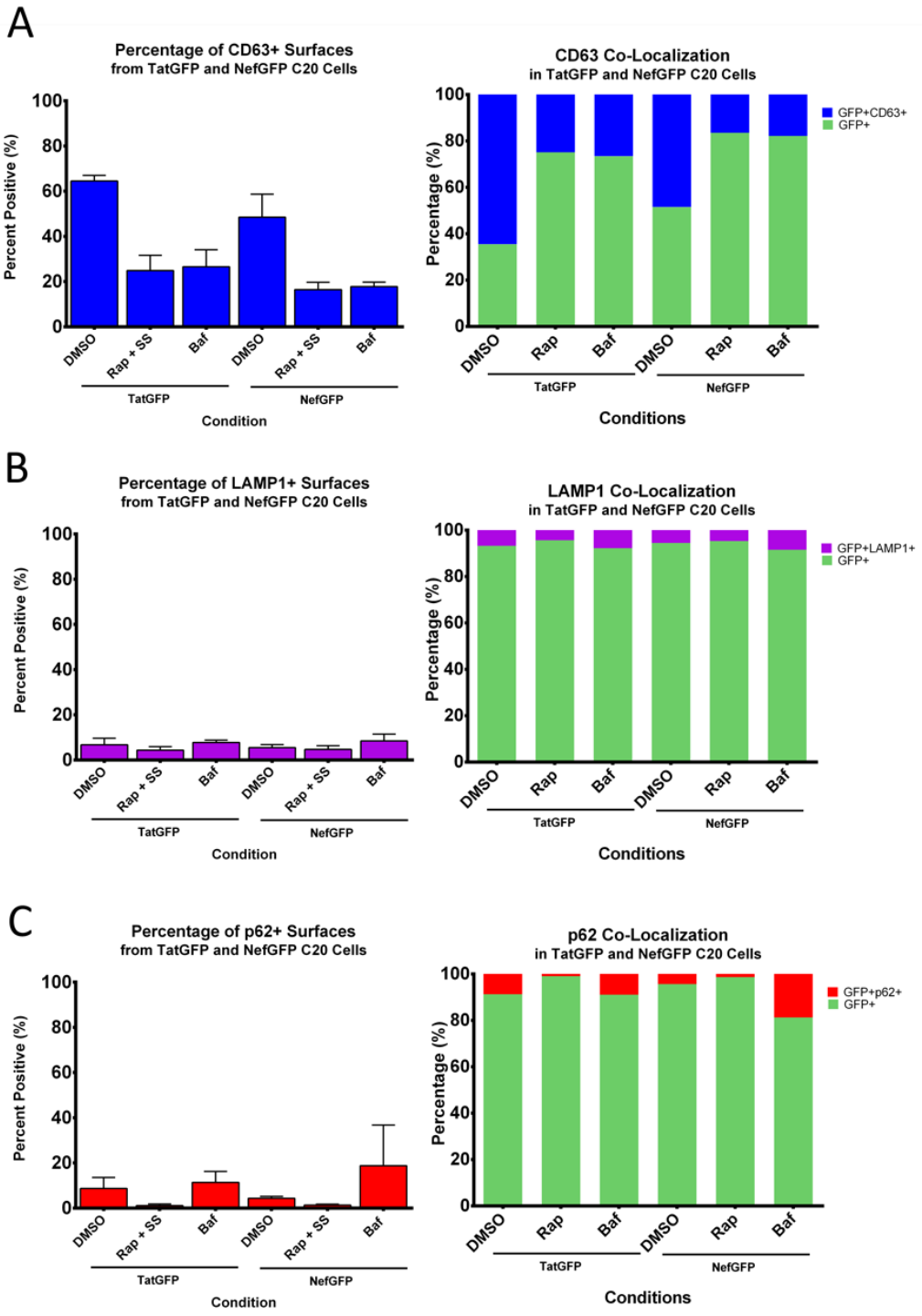

Figure 9. TatGFP and NefGFP C20 EV Co-Localization Data. The summation of co-localization data of three replicates, with the error bars showing the standard error of the mean. Graphs in the left-hand column show the percent positive surfaces for the marker of interest. Graphs in the right-hand column represent the summation of both the surfaces positive and negative for the marker of interest. **(A)** Co-localization with CD63. **(B)** Co-localization with LAMP1. **(C)** Co-localization with p62.

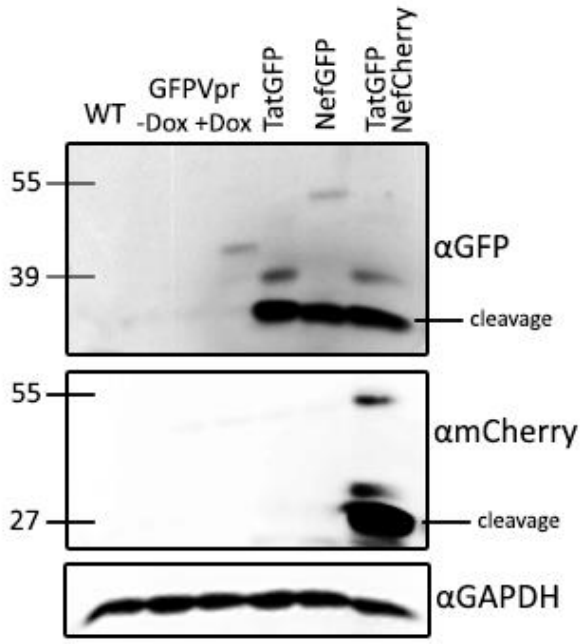

Figure 10. Western Blot of Transduced C20 Cells. This Western blot shows the successful transduction of the lentiviral vectors expressing the fluorescent HIV-1 protein fusions. Unfortunately, in these cells Tat-GFP, Nef-GFP, and Nef-mCherry appear to get cleaved quite frequently.

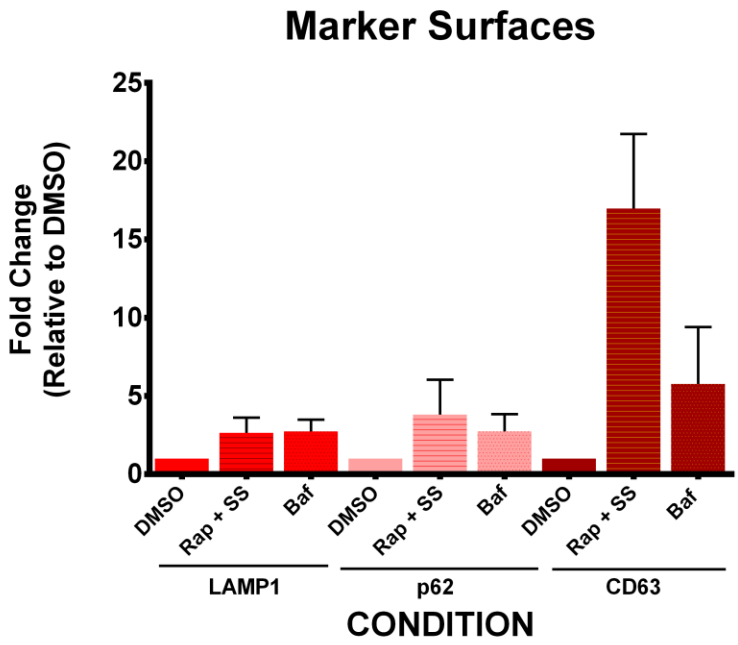

Figure 11. Fold Changes in EV Markers. This graph is the summation of three replicates and shows the fold changes of LAMP1, p62, and CD63 in EVs upon treatment with rapamycin and bafilomycin A1. Error bars report the standard error of the mean.

CHAPTER SIX

DISCUSSION

Analysis of EVs at an individual level has the potential to be a powerful tool as it allows the study of EVs without assuming homogeneity as so many other of the current methods do. The identification of distinct populations that carry dysregulated miRNAs and pathogenic proteins could be exploited as targets for therapy to eliminate the EV-mediated transfer of these components and their subsequent deleterious effects. Further analysis of such populations could provide valuable insight into how alteration in cargo loading in EVs, whether due to a microbial pathogen or as a consequence of cellular misfunction, leads to the appearance of these populations, and in turn, how they lead to various disease states, such as the manifestations of HAND. Beyond studies of pathology, these tools can be used on any cell type under any conditions to gain a deeper understanding of EV function and biogenesis in general.

Through the combination of wide-field deconvolution microscopy and a molecular beacon, I attempted to detect miR-21 in individual EVs. Unfortunately, this system needs to be heavily optimized before it can be validated as a method to identify miRNAs in EVs. The apparent detection of miR-21 in the absence of EV permeabilization was a surprising result as one would expect that the molecular beacon would not be able to detect the luminal miR-21 otherwise. A possible explanation is that the EVs are becoming leaky during the purification process, as the high speeds used in the ultracentrifugation steps to pellet and concentrate the

EVs can be potentially damaging.[104] While the spinoculation technique does not appear to damage viruses when spun onto cells,[109] spinning EVs directly onto glass may be another step where EVs are getting damaged. Another surprising result was the destructiveness of saponin and digitonin given that both, and much harsher detergents like Triton X-100, are regularly used to permeabilize EVs in other contexts. It is possible that the two detergents did not destroy the EVs and instead lead to the dissociation of the S15-GFP EV marker as it is not a transmembrane protein that would be resistant to such treatment. However, the decline in the beacon signal also observed in these samples may suggest that the EVs are being destroyed. This result is potentially tied to the methods used in these studies, as permeabilization of EVs with saponin, digitonin, or Triton X-100, are done for only a few minutes while this procedure necessitated that the EVs be in the presence of these detergents for 2 hours. On top of this longer co-incubation time, the high speeds of spinoculation while in the presence of these detergents may also be contributing to this loss of EVs.

The complete lack of co-localization of the S15-GFP marker and the molecular beacon signal was another unexpected result. It is important to remember, however, that S15-GFP is not a “pan-EV” marker meaning S15-GFP and miR-21 are potentially incorporated into completely different EV populations. The use of membrane-intercalating fluorescent dyes could be an improvement upon this method and provide better labelling of all EV populations. Alternatively, this result may be the product of damage to EVs either during isolation or spinoculation leading to the leakage of their luminal miRNAs.

The presence of molecular beacon signal in EVs isolated from miR-21 KO MSCs is perplexing. As mentioned earlier, this could either be the result of non-specific binding of the

beacon, or the beacon becoming linearized too easily. While the dual tagging of a molecular beacon with a fluorophore and a quencher makes it an ideal reporter construct, the small number of base pairs holding the stem-loop shape of the quenched state together could be easily disrupted and lead to a false-positive signal. An alternative to the molecular beacon could be what is classically used in *in situ* hybridization, a linear probe. While both probes may have their own advantages and disadvantages, comparison of the two probes in this system would be valuable in optimizing this assay.

Beyond these experimental modifications, beacon specificity and the limit of assay detection should have been further evaluated prior to attempting to use the beacon in our single vesicle analysis method. Comparing the signals of molecular beacons with different target sequences in cells or EVs would have provided insight into beacon specificity. The effect of fixation on beacon signal should have been investigated as well. Multiple ways to assess the limit of detection with this beacon using known amounts of miR-21 should have been performed to determine this assay's sensitivity.

It is well-accepted in the field that EVs can be derived from different biogenesis pathways, resulting in differences in cargo that can lead to differences in function and bioactivity.[52,64] However, apart from the well-characterized exosome biogenesis pathway and formation of MVBs, the mechanisms involved in these different pathways are poorly understood. Previous studies of HIV-1 proteins Tat, Nef, and Vpr with our single vesicle analysis method revealed high co-localization of these proteins with various markers that I believed indicated these HIV-1 proteins were incorporated into EV populations with different biogenesis pathways. These assumptions were tested by focusing on manipulation of one pathway first,

the unconventional autophagic secretion pathway. EV flux through this pathway was altered by treatment of cells with rapamycin or bafilomycin A1.

As anticipated alteration of autophagy lead to an increase in release of Tat EVs. However, Tat did not co-localize much with the potential markers for autophagic secretion, LAMP1 and p62. Furthermore, disruption of autophagy also lead to an increase in the release of Nef EVs, although consistently not as much as Tat EVs. Neither Tat nor Nef co-localized with LAMP1 or p62, and in cells in which Tat and Nef were co-expressed the two proteins frequently co-localized with each other. These data may suggest that these two HIV-1 proteins are not incorporated into EVs by separate biogenesis pathways, and it is unclear if these EVs are in fact being derived from the unconventional autophagic secretion pathway. Additionally, with the amount of cleavage product detected in C20 cells it is possible the EVs assessed in these studies contained free GFP and mCherry instead of the fusion proteins, thus rendering all analyses inconclusive. The observation that the amount of Tat-GFP signal increases consistently more than the increases in Nef-GFP/Cherry signals potentially indicates the EVs being measured do contain the fusion proteins, as there would be no reason GFP would be incorporated differently between the Tat-GFP and Nef-GFP cells or why GFP would be selectively incorporated over mCherry in the TatGFP-NefCherry cells. However, this has yet to be confirmed by Western blot as initial attempts have not been able to detect either the fusions or free fluorescent proteins in concentrated C20 EVs. It is likely that much larger cultures will be needed to collect enough EVs to get a high enough protein concentration to be detectable.

The most unexpected results came from the analysis of how the EV markers of interest changed upon rapamycin or bafilomycin A1 treatment. The two autophagic markers, LAMP1

and p62, did increase with both treatments but curiously this was not reflected in the co-localization data. LAMP1 co-localization with Tat and Nef remained relatively constant while p62 co-localization appeared to decrease upon rapamycin treatment but slightly increase with bafilomycin A1 treatment. Interestingly a similar result has been observed in a study of EVs containing α-synuclein in which p62 was found to be increased in these EVs upon bafilomycin A1 treatment, but not upon treatment with rapamycin.[99] However the increase in overall LAMP1 and p62 EVs pales in comparison to the near 20-fold increase in total CD63 positive EVs upon rapamycin treatment. While not as drastic as rapamycin, bafilomycin A1 also increased the amount of CD63. This result was perplexing, as CD63 is a marker of the classical MVB-exosome biogenesis pathway and was supposed to serve as the control marker, yet it changed more in response to altered autophagy than the autophagic markers. Upon reflection, it perhaps makes sense that CD63 would change as the unconventional autophagic secretion pathway does involve the formation of MVBs prior to their fusion with secretory autophagosomes.[96] Additionally, CD63 is found not only in endosomes but also lysosomes and bears another name, lysosomal-associated membrane protein-3 (LAMP3).[110] CD63 has also been reported to co-localize with the autophagic marker LC3-II, and an increase in the secretion of CD63 positive EVs upon alteration of autophagy has been noted in other studies.[110–112]

Even with this newfound appreciation of CD63's roles in both the endosomal and autophagic pathways, the co-localization data of Tat and Nef with CD63 is still baffling. Despite the large increase in total CD63 positive EVs upon treatment with rapamycin or bafilomycin A1, the amount of Tat/Nef-GFP positive EVs also positive for CD63 drastically drops from 40-60 percent to around 10-20 percent. And more confusing still, this reduction in co-localization with

CD63 appears to be mitigated when Tat and Nef are co-expressed. One thing that is clear, is that these EV biogenesis pathways cannot be so easily compartmentalized and studied in isolation as these different pathways appear to share various elements, suggesting a great deal of crosstalk between them.

In future studies it would be valuable to examine other EV markers that are believed to be specific for certain biogenesis pathways, and how they change upon alteration of autophagy. Proteins such as CD9, CD81, CD82, TSG101, ALIX, HSP70/HSC70, HSP90, and FLOT1 are some of the most common EV markers and generally associated with the classical MVB-exosome biogenesis pathway.[52,65] However, as mentioned earlier such proteins are not completely exclusive to this pathway as CD9, CD81, and TSG101 in particular have also been observed to also be at the plasma membrane.[52,64,65] As far as the characterization of EVs containing HIV-1 proteins, it would be worthwhile to optimize the doxycycline-inducible Vpr system to be able to study Vpr-containing EVs in these C20 cells. Given their interaction, co-expression of Vpr and HIV-1 Gag in cells might lead to the production of EVs more in line with those produced during actual HIV-1 infection of a cell,[108] and could therefore be a future improvement upon the current system since separating EVs and HIV-1 virions from virally infected cells still remains impossible. Further studies with these Tat and Nef expressing cells would require that the cell lines be remade with new linker regions between the fusions to eliminate the cleavage products observed, ensuring that 100 percent of the fluorescent signals detected are the complete fusion proteins.

It is also important to note that these proteins did not co-localize solely with the markers that were used to assign their biogenesis pathways. Each protein co-localized to some

degree with all the markers assessed in the previous study, which included CD9, CD63, CD81, TSG101, and LAMP1, and the assumption that the highest amount of co-localization with a certain marker pointed to a specific biogenesis pathway is clearly shaky at best. Lastly, it is important to address the limitations of the single vesicle analysis method. While the algorithms are created as unbiasedly as is possible, real signals are potentially being excluded by these algorithms. This is particularly true for markers detected by immunostaining, in which the background threshold of signal is determined by secondary only controls and may explain why the fusion proteins were so often negative for any of the markers tested. Additionally, the results of the immunostaining are only as good as the antibodies used. Fuller coverage of the total EVs might be achieved through lipophilic fluorescent dyes and when combined with immunostaining could provide more accurate assessments of marker co-localization and differences between EV populations.

In this thesis, *The Characterization of RNA Content and Biogenesis Pathways of Extracellular Vesicles That Have Been Implicated in the Pathogenesis of HIV-1 Associated Neurocognitive Disorder*s, I explored methods to characterize EVs in the hopes of gaining a better understanding of the EV populations that play a role in the pathogenesis of HAND. While it will require a lot of optimization to function properly and consistently, I took the first steps in the development of a method to detect miRNAs in individual EVs. I also attempted to resolve the biogenesis pathways of EVs containing the HIV-1 proteins Tat, Nef, and Vpr, and found that such processes are intricate and interconnected and cannot be simplified down to a handful of markers.

APPENDIX A

SUPPLEMENTARY FIGURES

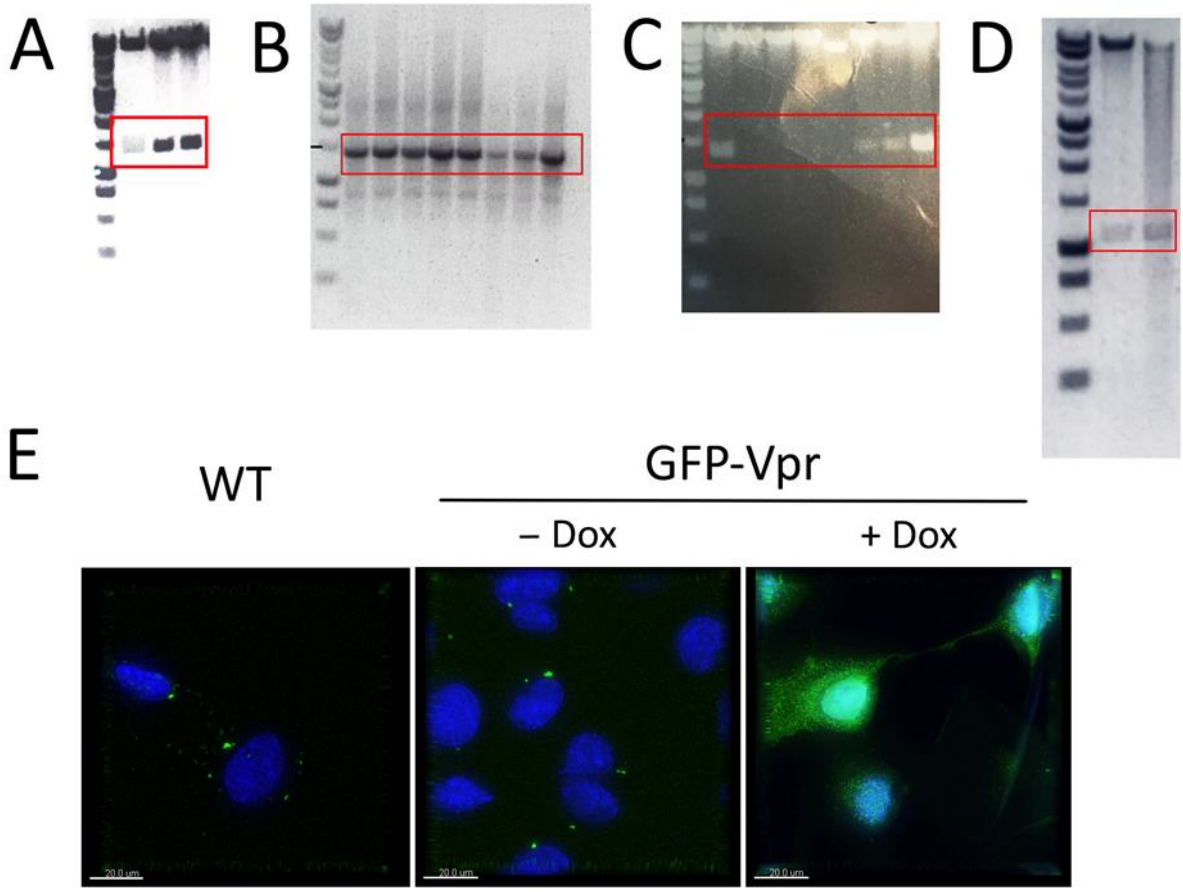

Supplementary Figure 1. Agarose Gels and Images of Generated Lentiviral HIV-1 Fusion Protein Plasmids. Panels A-D depict the results of agarose gel electrophoresis after enzyme digestion of isolated DNA, confirming the presence of the fusion proteins. **(A)** Nef-GFP-pLVX. **(B)** Nef-Cherry generated by SOEing PCR. **(C)** Nef-Cherry-pLVX. **(D)** GFP-Vpr-pLKO. **(E)** Fluorescence microscopy images showing the induction of GFP-Vpr in transduced C20 cells when in the presence of 500ng/mL doxycycline.

REFERENCE LIST

1. Arts, E. J. & Hazuda, D. J. HIV-1 antiretroviral drug therapy. *Cold Spring Harb. Perspect. Med.* **2,** (2012).

2. Watkins, C. C. & Treisman, G. J. Cognitive impairment in patients with AIDS - prevalence and severity. *HIV. AIDS. (Auckl).* **7,** 35–47 (2015).

3. McArthur, J. C., Steiner, J., Sacktor, N. & Nath, A. Human immunodeficiency virus-associated neurocognitive disorders mind the gap. *Ann. Neurol.* **67,** 699–714 (2010).

4. Heaton, R. K. *et al.* HIV-associated neurocognitive disorders persist in the era of potent antiretroviral therapy: Charter Study. *Neurology* **75,** 2087–2096 (2010).

5. Rock, R. B. *et al.* Role of Microglia in Central Nervous System Infections Role. *Clin. Microbiol. Rev.* **17,** 942–64 (2004).

6. Tavazzi, E., Morrison, D., Sullivan, P., Morgello, S. & Fischer, T. Brain Inflammation is a Common Feature of HIV-Infected Patients without HIV Encephalitis or Productive Brain Infection. *Curr. HIV Res.* **12,** 97–110 (2014).

7. Hubert, A. *et al.* Elevated Abundance, Size, and MicroRNA Content of Plasma Extracellular Vesicles in Viremic HIV-1+ Patients. *JAIDS J. Acquir. Immune Defic. Syndr.* **70,** 219–227 (2015).

8. Kadiu, I., Narayanasamy, P., Dash, P. K., Zhang, W. & Gendelman, H. E. Biochemical and Biologic Characterization of Exosomes and Microvesicles as Facilitators of HIV-1 Infection in Macrophages. *J. Immunol.* **189,** 744–754 (2012).

9. Madison, M. N. & Okeoma, C. M. Exosomes: Implications in HIV-1 pathogenesis. *Viruses* **7,** 4093–4118 (2015).

10. Narayanan, A. *et al.* Exosomes derived from HIV-1-infected cells contain trans-activation response element RNA. *J. Biol. Chem.* **288,** 20014–20033 (2013).

11. Bernard, M. A. *et al.* Novel HIV-1 MiRNAs stimulate TNFa release in human macrophages via TLR8 signaling pathway. *PLoS One* **9,** (2014).

12. Ellwanger, J. H., Veit, T. D. & Chies, J. A. B. Exosomes in HIV infection: A review and critical look. *Infect. Genet. Evol.* **53,** 146–154 (2017).

13. Rahimian, P. & He, J. J. HIV-1 Tat-shortened neurite outgrowth through regulation of microRNA-132 and its target gene expression. *J Neuroinflammation* **13,** 247 (2016).

14. Hu, G. *et al.* Exosome-mediated shuttling of microRNA-29 regulates HIV Tat and morphine-mediated Neuronal dysfunction. *Cell Death Dis.* **3,** e381 (2012).

15. Debaisieux, S., Rayne, F., Yezid, H. & Beaumelle, B. The Ins and Outs of HIV-1 Tat. *Traffic* **13,** 355–363 (2012).

16. Rahimian, P. & He, J. J. Exosome-associated release, uptake, and neurotoxicity of HIV-1 Tat protein. *J. Neurovirol.* **22,** 774–788 (2016).

17. James, T., Nonnemacher, M. R., Wigdahl, B. & Krebs, F. C. Defining the roles for Vpr in HIV-1-associated neuropathogenesis. *J. Neurovirol.* **22,** 403–415 (2016).

18. Bagashev, A. & Sawaya, B. E. Roles and functions of HIV-1 Tat protein in the CNS: an overview. *Virol. J.* **10,** 358 (2013).

19. Mangino, G. *et al.* HIV-1 myristoylated nef treatment of murine microglial cells activates inducible nitric oxide synthase, NO2production and neurotoxic activity. *PLoS One* **10,** 1–21 (2015).

20. Saribas, A. S., Khalili, K. & Sariyer, I. K. Dysregulation of autophagy by HIV-1 Nef in human astrocytes. *Cell Cycle* **14,** 2899–2904 (2015).

21. Sharp, P. M. & Hahn, B. H. Origins of HIV and the AIDS pandemic. *Cold Spring Harb. Perspect. Med.* **1,** 1–22 (2011).

22. UNAIDS. Fact sheet - Latest global and regional statistics on the status of the AIDS epidemic. *Unaids* 8 (2017). Available at: http://www.unaids.org/en/resources/fact-sheet.

23. Cohen, M. S., Shaw, G. M., McMichael, A. J. & Haynes, B. F. Acute HIV-1 Infection. *N. Engl. J. Med.* **364,** 1943–54 (2011).

24. Perreau, M., Levy, Y. & Pantaleo, G. Immune response to HIV. *Curr. Opin. HIV AIDS* **8,** 333–340 (2013).

25. Grill, M. F. & Price, R. W. *Central nervous system HIV-1 infection*. *Handbook of Clinical Neurology* **123,** (Elsevier B.V., 2014).

26. Zayyad, Z. & Spudich, S. Neuropathogenesis of HIV: from initial neuroinvasion to HIV-associated neurocognitive disorder (HAND). *Curr. HIV/AIDS Rep.* **12,** 16–24 (2015).

27. Williams, D. W. *et al.* Mechanisms of HIV Entry into the CNS: Increased Sensitivity of HIV Infected CD14+CD16+ Monocytes to CCL2 and Key Roles of CCR2, JAM-A, and ALCAM in Diapedesis. *PLoS One* **8,** 1–15 (2013).

28. Joseph, S. B., Arrildt, K. T., Sturdevant, C. B. & Swanstrom, R. HIV-1 target cells in the CNS. *J. Neurovirol.* **21,** 276–89 (2015).

29. Ballabh, P., Braun, A. & Nedergaard, M. The blood-brain barrier: An overview: Structure, regulation, and clinical implications. *Neurobiol. Dis.* **16,** 1–13 (2004).

30. Hong, S. & Banks, W. A. Role of the immune system in HIV-associated neuroinflammation and neurocognitive implications. *Brain. Behav. Immun.* **45,** 1–12 (2015).

31. Dohgu, S., Ryerse, J. S., Robinson, S. M. & Banks, W. A. Human immunodeficiency virus-1 uses the mannose-6-phosphate receptor to cross the blood-brain barrier. *PLoS One* **7,** 1–12 (2012).

32. Ghafouri, M., Amini, S., Khalili, K. & Sawaya, B. E. HIV-1 associated dementia: Symptoms and causes. *Retrovirology* **3,** 1–11 (2006).

33. Doitsh, G. *et al.* Cell death by pyroptosis drives CD4 T-cell depletion in HIV-1 infection. *Nature* **505,** 509–514 (2014).

34. Vella, S., Schwartländer, B., Sow, S. P., Eholie, S. P. & Murphy, R. L. The history of antiretroviral therapy and of its implementation in resource-limited areas of the world. *AIDS* **26,** 1231–1241 (2012).

35. Dybul, M. *et al.* Short-cycle structured intermittent treatment of chronic HIV infection with highly active antiretroviral therapy: effects on virologic, immunologic, and toxicity parameters. *Proc.Natl.Acad.Sci.U.S.A* **98,** 15161–15166 (2001).

36. Evering, T. H. *et al.* Absence of HIV-1 evolution in the gut-associated lymphoid tissue from patients on combination antiviral therapy initiated during primary infection. *PLoS Pathog.* **8,** (2012).

37. Hazuda, D. J. HIV integrase as a target for antiretroviral therapy. *Curr. Opin. HIV AIDS* **7,** 383–389 (2012).

38. Hong, F. F. & Mellors, J. W. Impact of Antiretroviral Therapy on HIV-1 Persistence: The Case for Early Initiation. *AIDS Rev.* **17,** 71–82 (2012).

39. Fonner, V. A. *et al.* Effectiveness and safety of oral HIV preexposure prophylaxis for all populations. *AIDS* **30,** 1973–83 (2016).

40. Mondy, K. & Tebas, P. Cardiovascular Risks of Antiretroviral Therapies. *Annu. Rev. Med.* **58,** 141–155 (2007).

41. Herrin, M. *et al.* Weight gain and incident diabetes among HIV-infected veterans initiating antiretroviral therapy compared with uninfected individuals. *J. Acquir. Immune Defic. Syndr.* **73,** 228–236 (2016).

42. Clifford, D. B. & Ances, B. M. HIV-associated neurocognitive disorder. *Lancet. Infect. Dis.* **13,** 976–86 (2013).

43. Letendre, S. L. *et al.* Enhancing antiretroviral therapy for human immunodeficiency virus cognitive disorders. *Ann. Neurol.* **56,** 416–423 (2004).

44. Bednar, M. M. *et al.* Compartmentalization, Viral Evolution, and Viral Latency of HIV in the CNS. *Curr. HIV/AIDS Rep.* **12,** 262–71 (2015).

45. Peluso, M. J. *et al.* Cerebrospinal fluid HIV escape associated with progressive neurologic dysfunction in patients on antiretroviral therapy with well controlled plasma viral load. *AIDS* **26,** 1765–1774 (2012).

46. Valcour, V., Sithinamsuwan, P., Letendre, S. & Ances, B. Pathogenesis of HIV in the central nervous system. *Curr. HIV/AIDS Rep.* **8,** 54–61 (2011).

47. Cysique, L. A. *et al.* Dynamics of cognitive change in impaired HIV-positive patients initiating antiretroviral therapy. *Neurology* **73,** 342–348 (2009).

48. Edelman, M. *et al.* Microglial nodule encephalitis: limited CNS infection despite disseminated systemic cryptococcosis. *Clin. Neuropathol.* **15,** 30–3 (1996).

49. Lanjewar, D. N., Jain, P. P. & Shetty, C. R. Profile of central nervous system pathology in patients with AIDS: an autopsy study from India. *AIDS* **12,** 309–313 (1998).

50. Fields, J. *et al.* HIV-1 Tat Alters Neuronal Autophagy by Modulating Autophagosome Fusion to the Lysosome: Implications for HIV-Associated Neurocognitive Disorders. *J. Neurosci.* **35,** 1921–1938 (2015).

51. Ojha, C. R. *et al.* Interplay between autophagy, exosomes and HIV-1 associated neurological disorders: New insights for diagnosis and therapeutic applications. *Viruses* **9,** 1–21 (2017).

52. Raposo, G. & Stoorvogel, W. Extracellular vesicles: Exosomes, microvesicles, and friends. *J. Cell Biol.* **200,** 373–383 (2013).

53. Simons, M. & Raposo, G. Exosomes--vesicular carriers for intercellular communication. *Curr. Opin. Cell Biol.* **21,** 575–581 (2009).

54. Gradilla, A. C. *et al.* Exosomes as Hedgehog carriers in cytoneme-mediated transport and secretion. *Nat. Commun.* **5,** (2014).

55. Komaki, M. *et al.* Exosomes of human placenta-derived mesenchymal stem cells stimulate angiogenesis. *Stem Cell Res. Ther.* **8,** 1–12 (2017).

56. Danilchik, M. & Tumarkin, T. Exosomal trafficking in Xenopus development. *Genesis* **55,** 1–7 (2017).

57. Lee, C. *et al.* Exosomes Mediate the Cytoprotective Action of Mesenchymal Stromal Cells on Hypoxia-Induced Pulmonary Hypertension. *Circulation* **126,** 2601–2611 (2012).

58. Madison, M. N., Jones, P. H. & Okeoma, C. M. Exosomes in human semen restrict HIV-1 transmission by vaginal cells and block intravaginal replication of LP-BM5 murine AIDS virus complex. *Virology* **482,** 189–201 (2015).

59. Robbins, P. D. & Morelli, A. E. Regulation of Immune Responses by Extracellular Vesicules. *Nat. Immunol.* **14,** 195–208 (2014).

60. Rajendran, L. *et al.* Alzheimer's disease beta-amyloid peptides are released in association with exosomes. *Proc. Natl. Acad. Sci.* **103,** 11172–11177 (2006).

61. Danzer, K. M. *et al.* Exosomal cell-to-cell transmission of alpha synuclein oligomers. *Mol. Neurodegener.* **7,** 42 (2012).

62. Rak, J. Microparticles in Cancer. *Semin. Thromb. Hemost.* **36,** 888–906 (2010).

63. Hood, J. L., San Roman, S. & Wickline, S. A. Exosomes released by melanoma cells prepare sentinel lymph nodes for tumor metastasis. *Cancer Res.* **71,** 3792–3801 (2011).

64. Akers, J. C., Gonda, D., Kim, R., Carter, B. S. & Chen, C. C. Biogenesis of extracellular vesicles (EV): exosomes, microvesicles, retrovirus-like vesicles, and apoptotic bodies. *J. Neurooncology* **113,** 1–11 (2013).

65. Abels, E. R. & Breakefield, X. O. Introduction to Extracellular Vesicles: Biogenesis, RNA Cargo Selection, Content, Release, and Uptake. *Cell. Mol. Neurobiol.* **36,** 301–312 (2016).

66. Crescitelli, R. *et al.* Distinct RNA profiles in subpopulations of extracellular vesicles: Apoptotic bodies, microvesicles and exosomes. *J. Extracell. Vesicles* **2,** 1–10 (2013).

67. Andreu, Z. & Yáñez-Mó, M. Tetraspanins in extracellular vesicle formation and function. *Front. Immunol.* **5,** 1–12 (2014).

68. Hon, K. W., Abu, N., Ab Mutalib, N.-S. & Jamal, R. Exosomes As Potential Biomarkers and Targeted Therapy in Colorectal Cancer: A Mini-Review. *Front. Pharmacol.* **8,** 1–8 (2017).

69. Cheng, L., Sharples, R. A., Scicluna, B. J. & Hill, A. F. Exosomes provide a protective and enriched source of miRNA for biomarker profiling compared to intracellular and cell-free blood. *J. Extracell. Vesicles* **3,** 1–14 (2014).

70. Bartel, D. P. MicroRNAs: Genomics, Biogenesis, Mechanism, and Function. *Cell* **116,** 281–297 (2004).

71. Hammond, S. M. An overview of microRNAs. *Adv. Drug Deliv. Rev.* **87,** 3–14 (2015).

72. Mukerjee, R. *et al.* Deregulation of microRNAs by HIV-1 Vpr protein leads to the development of neurocognitive disorders. *J. Biol. Chem.* **286,** 34976–34985 (2011).

73. Croce, C. M. MicroRNA dysregulation in acute myeloid leukemia. *J. Clin. Oncol.* **31,** 2065–2066 (2013).

74. Brites, D. & Fernandes, A. Neuroinflammation and Depression: Microglia Activation, Extracellular Microvesicles and microRNA Dysregulation. *Front. Cell. Neurosci.* **9,** 1–20 (2015).

75. Gupta, A. & Pulliam, L. Exosomes as mediators of neuroinflammation. *J. Neuroinflammation* **11,** 1–10 (2014).

76. Aqil, M. *et al.* The HIV Nef protein modulates cellular and exosomal miRNA profiles in human monocytic cells. *J. Extracell. Vesicles* **3,** 1–11 (2014).

77. Goedert, M. Alzheimer's and Parkinson's diseases: The prion concept in relation to assembled Aβ, tau, and α-synuclein. *Science (80-.).* **349,** 61–69 (2015).

78. Steiner, J. A., Angot, E. & Brundin, P. A deadly spread: Cellular mechanisms of α-synuclein transfer. *Cell Death Differ.* **18,** 1425–1433 (2011).

79. Fang, Y. *et al.* Higher-order oligomerization targets plasma membrane proteins and HIV Gag to exosomes. *PLoS Biol.* **5,** 1267–1283 (2007).

80. Dujardin, S. *et al.* Ectosomes: A new mechanism for non-exosomal secretion of Tau protein. *PLoS One* **9,** 28–31 (2014).

81. Polanco, J. C., Scicluna, B. J., Hill, A. F. & Gï¿½tz, J. Extracellular vesicles isolated from the brains of rTg4510 mice seed tau protein aggregation in a threshold-dependent manner. *J. Biol. Chem.* **291,** 12445–12466 (2016).

82. Yelamanchili, S. V., Datta Chaudhuri, A., Chen, L. N., Xiong, H. & Fox, H. S. MicroRNA-21 dysregulates the expression of MEF2C in neurons in monkey and human SIV/HIV neurological disease. *Cell Death Dis.* **1,** e77-11 (2010).

83. Mishra, R., Chhatbar, C. & Singh, S. K. HIV-1 Tat C-mediated regulation of tumor necrosis factor receptor-associated factor-3 by microRNA 32 in human microglia. *J. Neuroinflammation* **9,** 1–15 (2012).

84. Zeitler, M., Steringer, J. P., Möller, H. M., Mayer, M. P. & Nickel, W. HIV-Tat protein forms phosphoinositide-dependent membrane pores implicated in unconventional protein secretion. *J. Biol. Chem.* **290,** 21976–21984 (2015).

85. Fanales-Belasio, E. *et al.* Native HIV-1 Tat protein targets monocyte-derived dendritic cells and enhances their maturation, function, and antigen-specific T cell responses. *J Immunol* **168,** 197–206 (2002).

86. Liu, J. *et al.* HIV-1 Tat Protein Increases Microglial Outward K+ Current and Resultant Neurotoxic Activity. *PLoS One* **8,** (2013).

87. Krogh, K. A., Green, M. V & Thayer, S. A. HIV-1 Tat-induced changes in synaptically-driven network activity adapt during prolonged exposure Kelly. *Curr. HIV Res.* **12,** 406–414 (2015).

88. Basmaciogullari, S. & Pizzato, M. The activity of Nef on HIV-1 infectivity. *Front. Microbiol.* **5,** 1–12 (2014).

89. Shen, B., Wu, N., Yang, M. & Gould, S. J. Protein targeting to exosomes/microvesicles by plasma membrane anchors. *J. Biol. Chem.* **286,** 14383–14395 (2011).

90. Aqil, M., Naqvi, A. R., Bano, A. S. & Jameel, S. The HIV-1 Nef Protein Binds Argonaute-2 and Functions as a Viral Suppressor of RNA Interference. *PLoS One* **8,** 1–11 (2013).

91. Lenassi, M. *et al.* HIV Nef is Secreted in Exosomes and Triggers Apoptosis in Bystander CD4+ T Cells. *Traffic* **11,** 110–122 (2010).

92. Leymarie, O., Lepont, L. & Berlioz-Torrent, C. Canonical and Non-Canonical Autophagy in HIV-1 Replication Cycle. *Viruses* **9,** 270 (2017).

93. Khan, M. *et al.* Nef exosomes isolated from the Plasma of Individuals with HIV-Associated Dementia (HAD) can induce Aβ1–42 Secretion in SH- SY5Y Neural cells. *J. Neurovirol.* **3,** 973–982 (2016).

94. Le Rouzic, E. & Benichou, S. The Vpr protein from HIV-1: Distinct roles along the viral life cycle. *Retrovirology* **2,** 1–14 (2005).

95. Gould, S. J. & Raposo, G. As we wait: Coping with an imperfect nomenclature for extracellular vesicles. *J. Extracell. Vesicles* **2,** 3–5 (2013).

96. Ponpuak, M. *et al.* Secretory autophagy. *Curr. Opin. Cell Biol.* **35,** 106–116 (2015).

97. Nickel, W. & Rabouille, C. Mechanisms of regulated unconventional protein secretion. *Nat. Rev. Mol. Cell Biol.* **10,** 148–155 (2009).

98. Cadwell, K. & Debnath, J. Beyond self-eating: The control of nonautophagic functions and signaling pathways by autophagyrelated proteins. *J. Cell Biol.* **217,** 813–822 (2018).

99. Minakaki, G. *et al.* Autophagy inhibition promotes SNCA/alpha-synuclein release and transfer via extracellular vesicles with a hybrid autophagosome-exosome-like phenotype. *Autophagy* **14,** 98–119 (2018).

100. Eitan, E., Suire, C., Zhang, S. & Mattson, M. P. Impact of lysosome status on extracellular vesicle content and release. *Ageing Res. Rev.* **32,** 65–74 (2016).

101. Mhlanga, M. M., Vargas, D. Y., Fung, C. W., Kramer, F. R. & Tyagi, S. tRNA-linked molecular beacons for imaging mRNAs in the cytoplasm of living cells. *Nucleic Acids Res.* **33,** 1902–1912 (2005).

102. Lee, J. H., Kim, J. A., Kwon, M. H., Kang, J. Y. & Rhee, W. J. In situ single step detection of exosome microRNA using molecular beacon. *Biomaterials* **54,** 116–125 (2015).

103. Campbell, E. M., Perez, O., Melar, M. & Hope, T. J. Labeling HIV-1 virions with two fluorescent proteins allows identification of virions that have productively entered the target cell. *Virology* **360,** 286–93 (2007).

104. Li, P., Kaslan, M., Lee, S. H., Yao, J. & Gao, Z. Progress in Exosome Isolation Techniques. *Theranostics* **7,** 789–804 (2017).

105. Sekar, D. *et al.* Role of MicroRNA 21 in Mesenchymal Stem Cell (MSC) Differentiation: A Powerful Biomarker in MSCs Derived Cells. *Curr. Pharm. Biotechnol.* **16,** 43–48 (2015).

106. Eskelinen, E. L. Roles of LAMP-1 and LAMP-2 in lysosome biogenesis and autophagy. *Mol. Aspects Med.* **27,** 495–502 (2006).

107. Huynh, K. K. *et al.* LAMP proteins are required for fusion of lysosomes with phagosomes. *EMBO J.* **26,** 313–324 (2007).

108. Chutiwitoonchai, N. *et al.* HIV-1 Vpr abrogates the effect of TSG101 overexpression to support virus release. *PLoS One* **11,** 1–17 (2016).

109. O'Doherty, U., Swiggard, W. J. & Malim, M. H. Human Immunodeficiency Virus Type 1 Spinoculation Enhances Infection through Virus Binding. *J. Virol.* **74,** 10074–10080 (2000).

110. Ushio, H. *et al.* Crucial role for autophagy in degranulation of mast cells. *J. Allergy Clin. Immunol.* **127,** 1267–1276 (2011).

111. Hurwitz, S. N., Cheerathodi, M. R., Nkosi, D., York, S. B. & Meckes, D. G. Tetraspanin CD63 Bridges Autophagic and Endosomal Processes To Regulate Exosomal Secretion and Intracellular Signaling of Epstein-Barr Virus LMP1. *J. Virol.* **92,** e01969-17 (2017).

112. Poehler, A. M. *et al.* Autophagy modulates SNCA/α-synuclein release, thereby generating a hostile microenvironment. *Autophagy* **10,** 2171–2192 (2014).

VITA

The author, Virginia Zwikelmaier, was born in Saint Louis, Missouri on October 5, 1991 to Kurt and Madeline Zwikelmaier. She attended Colorado State University in Fort Collins, Colorado where she earned a Bachelor of Science in Biochemistry in May 2014. In 2016, Virginia matriculated into the Loyola University Chicago Stritch School Infectious Disease and Immunology Graduate Program and began her graduate education under the mentorship of Dr. Edward Campbell. After completion of her graduate studies, Virginia will pursue employment in industry.